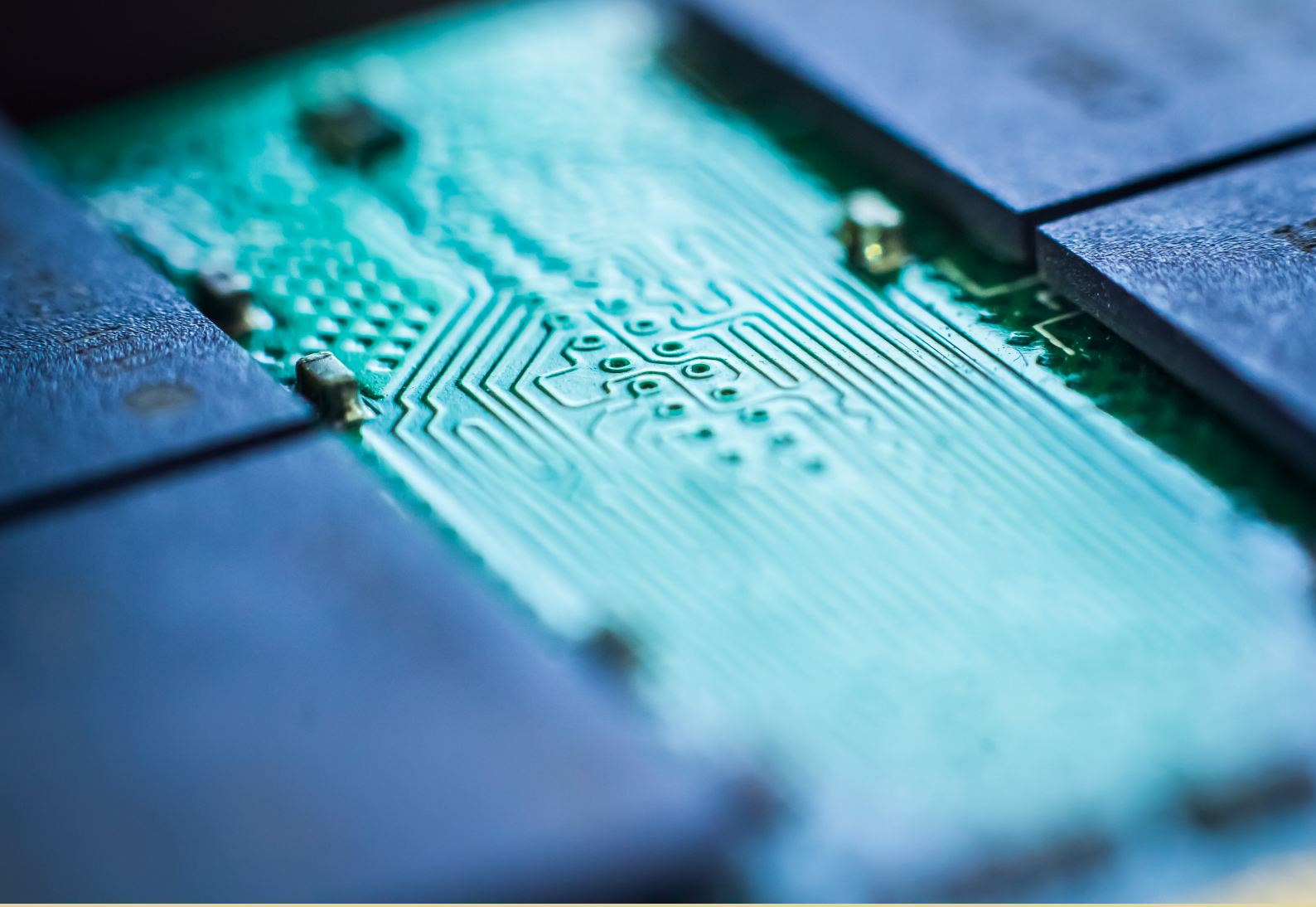

Sara da Fonte Anjo

THE ELECTRICAL IMPEDANCE SPECTROSCOPY TECHNIQUE – 3 CASE STUDIES IN CHEMICAL AND BIOLOGICAL MATERIALS.

Thesis submitted to the University of Coimbra for compliance with the requirements for the degree of Master in Biomedical Engineering under the scientific supervision of Full Professor Carlos Manuel Bolota Alexandre Correia (UC).

September 2016

· U C ·

Universidade de Coimbra

• U  C •

FCTUC FACULDADE DE CIÊNCIAS
E TECNOLOGIA
UNIVERSIDADE DE COIMBRA

Integrated Master in Biomedical Engineering

The Electrical Impedance Spectroscopy Technique – 3 Case Studies in chemical and biological materials.

Thesis submitted to the University of Coimbra for compliance with the requirements for the degree of Master in Biomedical Engineering

Author:

Sara da Fonte Anjo

Supervisor:

Full Professor Carlos Correia

Co-Supervisors:

Pre-Bologna BSc. Tiago Marçal

Coimbra, 2016

Collaborators

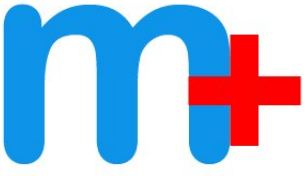

Aos meus pais...

Porque sem vocês nada disto seria possível!

Agradecimentos

Gostaria de agradecer ao Prof. Dr. Carlos Correia pelo apoio incondicional, pela paciência e pela disponibilidade contínua; ao GRANDE Tiago Marçal e ao Pedro Vaz por me terem aturado estes meses e terem amparado algumas quedas; ao Prof. Dr. Requicha Ferreira por todo o apoio na concessão dos protótipos. Um especial agradecimento à Dra. Ana Dias (*DEQ*), à Dra. Helena Teixeira e Dra. Paula Monsanto (*INML.CF*) pelo apoio prestado e plena disponibilidade. Agradeço ao Eng. Vitorino (*LOGOPLASTE*) pelo apoio prestado. Um especial "obrigada" ao Eng. Vitor Correia por todo o apoio desde o primeiro ano de faculdade.

Agradeço aos meus pais pela paciência, compreensão e apoio em tudo o que foi possível ao longo destes 23 anos – apesar da distância o amor torna tudo mais perto. Ao meu irmão, cunhada e pirralhos pelos bons momentos e por acreditarem em mim; Às tias, por tudo o que fazem por mim; Ao Pedrinho Rochinha por me apoiar nos momentos mais difíceis e nunca me deixar desistir ou baixar os braços, meu peixinho de arrastão. Aos meus amigos que ao longo destes 5 anos partilharam comigo momentos únicos que nunca esquecerei! Obrigada Diana Lourenço, minha para sempre colega de casa, pequena Ritinha por todos os bons momentos. Obrigada Shilli, Goubas, Nuni, Tó, Parma, Dux, Barote, Pandas e Sá, porque são especiais e vão sê-lo para sempre! Obrigada Iolanda e João Pereira pelo *LEDViser*! *Sardas*, vocês são especiais! Obrigada pelos inúmeros ombros amigos. Somos uma família para sempre! Ficam no coração. Obrigada Filipa, Catarina e Gininha pela amizade e apoio, mesmo quando só nos vemos uma vez por mês.

Abstract

Innovation is currently the most common word in scientific publications. The day life lack of time is responsible for the need of quick and accurate methods to solve problems. Three areas of interest arose: public health, related to waste water contaminants quick detection is needed; plastic industry with the need of maximum plastic bottles quality and its required accurate moisture quantifier to set if the Polyethylene Terephthalate (PET) pellets need to be dried; medical instrumentation with the need to detect the presence of *Plasmodium Falciparum* in blood samples to rapid diagnosis of malaria disease which had an incidence estimated in 200 million cases in 2013.

The aim of this project is to develop a portable, easy to use and accurate system, that presents also high sensibility to: waste-water contamination study; access the PET drying necessity; hemozoin detection. This device must be relatively cheap and easily replicated. To meet the above requirements, the method under study is based on Electrical Impedance Spectroscopy (EIS).

During the last decade, investigation in these three areas promoted the creation of innovative methods. The advantage of the device under study compared to the methods currently used are the low price associated and the low level of skills required. This properties makes it suitable to be used without place and price worries. EIS revealed to be an accurate method in order to distinguish material composition for the cases under study. Future work is expected to turn the device portable and autonomous.

Resumo

Nos dias de hoje, inovação é a palavra mais comum em publicações científicas. A velocidade de evolução do mundo atual torna necessário o desenvolvimento de métodos rápidos e precisos para resolução de vários problemas. Surgiram três áreas de interesse: saúde pública, onde surge a necessidade de um método rápido para deteção de contaminantes em águas residuais; indústria de garrafas de plástico, onde é necessário garantir a secagem dos peletes de Polyethylene Terephthalate (PET) antes da sua intrusão; instrumentação médica onde surge a necessidade de um dispositivo que detete *Plasmodium Falsiparum* em sangue infectado com malária, doença que afetou cerca de 200 milhões de pessoas em 2013.

O objetivo deste projeto é desenvolver um sistema portátil, preciso e fácil de usar e que apresente também alta sensibilidade a: estudo de contaminação de águas residuais; determinação da necessidade de secagem do PET; deteção de malária em sangue. Este sistema deve ser barato e replicável. Para isso o método em estudo é baseado em Espectroscopia de Impedância Elétrica (EIE).

Na última década foram investigados imensos métodos inovadores nestas áreas. A vantagem do dispositivo em estudo comparativamente com os métodos utilizados atualmente são o baixo preço e baixas habilitações técnicas necessárias ao utilizador. Estas propriedades tornam-no apropriado para qualquer terreno a um preço acessível. A EIE revelou ser um método preciso para distinguir a composição dos materiais em estudo. O objetivo futuro é tornar este dispositivo portátil e autónomo.

Acronyms

DC	Direct Current
EIS	Electrical Impedance Spectroscopy
INML	National Institute of Forensic Medicine
PBS	Peripheral Blood Smear
PCR	Polymerase Chain Reaction
PE	Polyethylene
PET	Polyethylene Terephthalate
PLA	Polylactic Acid
PSW	Plastic Solid Waste
RBC	Red Blood Cells
RDT	Rapid Diagnostic Test
RHDPE	Recycled High Density Polyethylene
STP	Sewage Treatment Plants
UHPLC	Ultra High-Performance Liquid Chromatography
WHO	World Health Organization

Chemical Elements

B	Boron
Ca	Calcium
Cl	Chlorine
Co	Cobalt
Cu	Copper
Fe	Iron
Mb	Molybdenum
Mg	Magnesium
Mn	Manganese
N	Nitrogen
Na	Sodium
O	Oxygen
P	Phosphor
S	Sulfur
Si	Silicon
V	Vanadium
Zn	Zinc

List of Figures

List of Tables

Contents

Chapter 1

Introduction

The purpose of this thesis and the main objective will be summarized in this section. The motivation for this study will be presented here. With the project progresses the interest in three topics arose. Thus an introduction on these topics will be presented being them: water contamination; PET pellets moisture; and the malaria disease. After this introduction, our experimental approach will be presented. Finally some system requirements and constrains are revealed.

1.1 Motivation

In the everyday life, **innovation** is one of the most common words in scientific publications. The soaring industrial development connected with the huge communication speed are affecting the communities at socio-economic levels. The constant and fast changes in the society, lead to the need of devices that support the lack of time and space which evolution heightens constantly. Nowadays, everything is expected to be always available no matter where or when. It has to answer all the requirements almost instantaneously. Thus we study a traditional technique in order to solve problems from distinct scopes – EIS.

The simplicity of the impedance study method and the fact of enable the use of a less expensive device compared to the ones actually used, with possibility of an easy transportation makes it able to be used anywhere turning it attractive for various applications.

Impedance measures are very sensitive to small electrochemical variations, what stim-

ulates us to take this study deeply, in order to find a solution to the problems encountered in each of the areas this thesis will focus: public health – waste-water contaminants study; plastics recycling industry – PET moisture; and medical instrumentation – malaria disease.

1.1.1 Water Contamination

Water is considered the most precious element of life. Primitive civilizations had no hygiene and sewage cares and waste water was simply thrown out. The lack of treatment promoted the creation of insects and rodents, proliferating diseases very easily.

Sewage Treatment Plants (STP) were created to collect population's waste water and to start the depollution of watercourses. This water gets into appropriate channels for being transported to the treatment system. After passing by micro-organisms purification systems with several steps (heating, hardness and corrosive agents correction, decantation, filtration, chlorination), it is released to enter the water cycle and get back to public supply, through a river, sea or lake. The schematic of a STP is presented in Figure 1.1. It shows the primary, secondary and tertiary treatment processes. First of all the flow is controlled and odours are pre-treated. Starting the primary treatment, solids in suspension and organic compounds are filtered. The fluid is decanted and screened to separate liquid from sediments which will also be processed before forwent. Then the fluid follows to the secondary process for solute removal and disinfection. All the solids and organic compounds in suspension which passed through primary treatment are now extracted by activated sludge and sedimentation system. The tertiary treatment is the most advanced neutralization system using biorreactors to remove undesirable ions and microorganisms. After this treatments the fluid is almost potable water [1].

When water treatment is not efficient and contaminated water returns to the environment it may result in infectious intestinal diseases [1].

This evidences proves the importance of performing water tests in the STP way out in order to ensure only harmless water is released to the environment [2].

Thus the STP effluent is analysed in order to quantify: Main elements (Ca, Mg, Na, Fe II and III, Cl , SO_4, SO_3, carbonate and bicarbonate ions); Minor elements (compound N, P and Si); Trace elements (B, Co, Cu, Fe, Mn, Mb, V, and Zn); Organic substances,

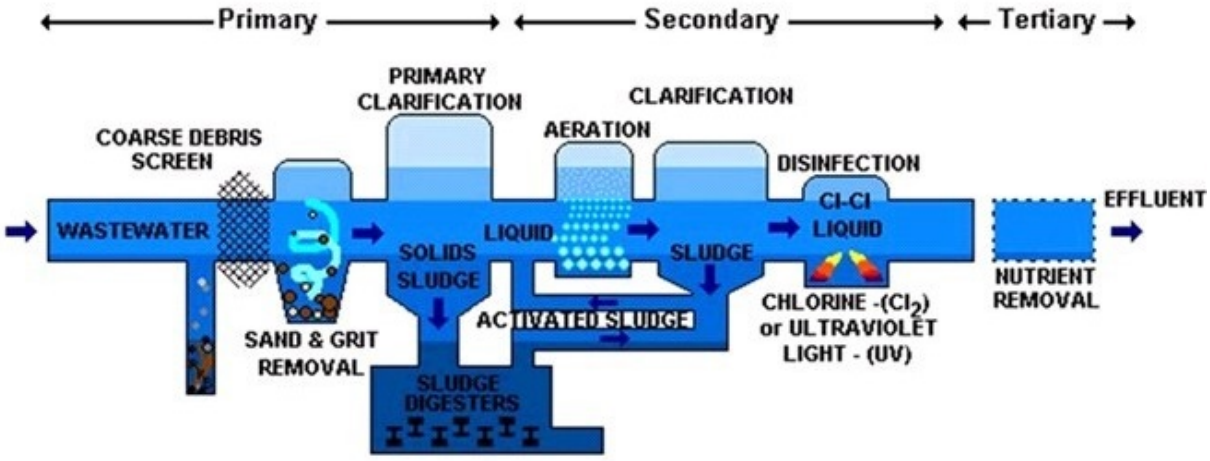

Figure 1.1: During primary treatment waste water suffers physical care for solids removal. Secondary treatment is biological in order to remove smaller organic compounds. Tertiary treatment attacks the microorganisms and cleans the water almost till potable water state by using reactors [1].

biochemical and chemical lack of oxygen; dissolved gases (O_2, N_2, CO_2, H_2 and CH_4); pH, red-ox potential, conductivity, total acidity and CO_2, alkalinity. [2, 3].

All methods developed for water ionic components determination in STP's are based on chemical reactions and with complex devices.

1.1.2 PET Moisture

Environmental concerns lead world's population to be aware for recycling needs. With scarcity of resources this practice is becoming increasingly common. Only China imports around 7 million tonnes of polymeric pellets per year in order to create new products from recycled Plastic Solid Waste (PSW). During the last 10 years, PET recycling increased 1200% [4]. Thus in addition to withstand temperature variations, recycled plastic must be resistant to external forces and impacts as well as to microbial attack [5]. Nonetheless it is intended that a recycled plastic keeps the physical/chemical and mechanical properties and the expected quality of a virgin material. In actual industry the main interest is in the abundant use of PET [4, 6, 7].

PET is a saturated polyester and represents a huge slice of the actual plastic industry due to its thermoplastic and mechanical properties. Its low density combined with the

stiffness and high shock resistance turns it perfect for a wide spectrum of applications. PET has several uses such as water bottles, textile fibres, bricolage utensils, hermetic packaging, bottle stoppers, kitchenware, brooms and cleaning utensils, handbags among others. PET has also low permeability for CO_2 and O_2 which protects its content from oxidation reactions and deterioration.

Its molecular formula is $C_{18}H_{22}N_4O_3$, and it is represented in Figure 1.2. It has a molecular weight of 342.39 g/mol. It is a polymeric polar resin which presents a dielectric constant ϵ_r ranges between 2,5 and 3. This property brings the material storage capacity of electric charges. It depends on the material composition and also on the frequency and voltage applied.

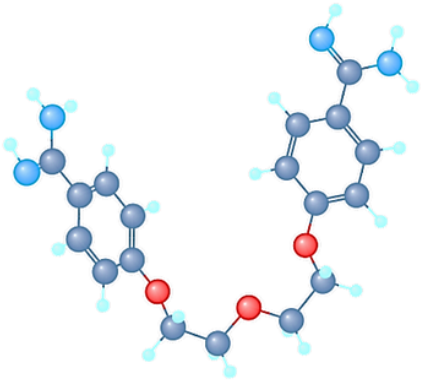

Figure 1.2: Representation of the PET molecule in three dimensions. Each sphere represents an atom: red spheres for the Oxygen, grey spheres for the Carbon, blue spheres for the Azote and light blue spheres for the Hydrogen [8].

After its life cycle, PET can pass through mechanical or feedstock recycling, incineration with energy recovery or land filling mentioned respectively in the likely order given to the ecological and economic level of the material recovery processes. First of all the collected plastic is clipped. Secondly, plastic is washed away to remove solid impurities and then it is separated by its density. Thirdly it is milled together and compacted with pieces of the same weight. Finally, it is then rewashed and sintered. At this stage the material can be stored or it suffers extrusion and quenching with cold water to form granules for commercialization [9, 10]. The plastic is typically converted by mechanical moulding methods such as extrusion, injection, blow, vacuum or inflation.

PET Higroscopy

PET is an hygroscopic material like most of the thermoplastics. This characteristic reflects the ease at which the material is able to adsorb and absorb the water present in the surrounding environment [11].

The presence of water between the polymer molecules causes a molecular reaction - hydrolysis - while the plastic pellets are melting. Hydrolysis interferes with the polymeric structure by decreasing the chains size causing lower molecular weight.

This results in lower resistance and tensile strength which does not allow the final quality required in the control. Most of hygroscopic plastics drying techniques are based on a dried air stream at high temperatures. For acceptable results, the water content on the plastics must be lower than 300 ppm (parts per million) [12, 13].

1.1.3 Malaria Disease

Malaria is an endemic disease affecting more than 200 million people per year. Although getting lower incidence, more than 400 000 deaths caused by malaria were registered in 2015, being 90 % of them in African region, according to World Health Organization (WHO). It remains the major cause of death in tropical and subtropical children and pregnant women [14].

Malaria is a disease caused by the infection of *Plasmodium falciparum* that gets in the blood circulation after a mosquito bite. This parasite is responsible for the conversion of hemoglobin of Red Blood Cells (RBC) in crystalline structures with different properties – hemozoin [15–17].

The illness is expressed by high fever and other flu effects, culminating in confusion, anaemia, breathing difficulties or even coma. When these effects occur and there is suspicion of this disease, laboratory tests are performed to screen malaria. The use of accurate Rapid Diagnostic Tests (RDT's) is crucial to detect early stages and prevent malaria's evolution, decreasing the tremendous number of deaths [14].

The lack of a robust RDT represents a huge problem in underdeveloped countries and, simultaneously, a research challenge [18, 19].

This study aims to detect Malaria with a less invasive method. It starts with the

study of small blood samples aiming to achieve a non-invasive probe.

Blood analysis

The primary object of study for malaria case is the human blood. Blood contains various figurative elements (erythrocytes, leukocytes and platelets), suspended in a serum which comprises more than half of the total volume of blood - the plasma (composed by water, proteins, nutrients, hormones and enzymes, as well as cellular metabolism products) [20].

Erythrocytes also known as RBC are the element present in greater amounts in the blood. There are about 5 million RBC's per cubic millimetre, in the blood of an adult and healthy man. Erythrocytes are composed of hemoglobin, ions, water, glucose and enzymes. Hemoglobin is the main component of erythrocytes. It has the function of oxygen transportation to the different tissues of the human body. It also carries a small amount of carbon dioxide [20].

When considering laboratory tests, blood is typically collected in small quantities and these components are analysed.

Hemozoin Formation

All the parasite infection starts with a mosquito bite. The spread of the parasite cycle is represented in Figure 1.3 and described below.

In the liver, *plasmodium* sporozoites develops in 3 states cycle. Firstly it forms the ring-tropozoite (first 24 hours) with the first nuclear division: hemoglobin degradation starts. The hemozoin is naturally synthesized within the digestive vacuoles of intraerythrocytic parasites. The parasite attacks hemoglobin heme (Fe^{2+}), releasing a ferrous group, yielding Fe^{3+} (protoporphyrin IX). Secondly the first mitosis occurs (schizont formation – between the 24^{th} and the 30^{th} hours) combined with the increase in hemoglobin degradation – crystallization of heme. Thirdly successive nuclear divisions take place and hemozoin, an insoluble crystal with paramagnetic properties, is obtained. It culminates with erythrocyte membrane rupture (followed by schizont segmentation). After this cycle, 16-32 merozoites are free to invade more erythrocytes [16, 22–24].

When another mosquito comes and gets both sexual forms of *plasmodium* - the gametocytes - that combined will form a new sporozoite.

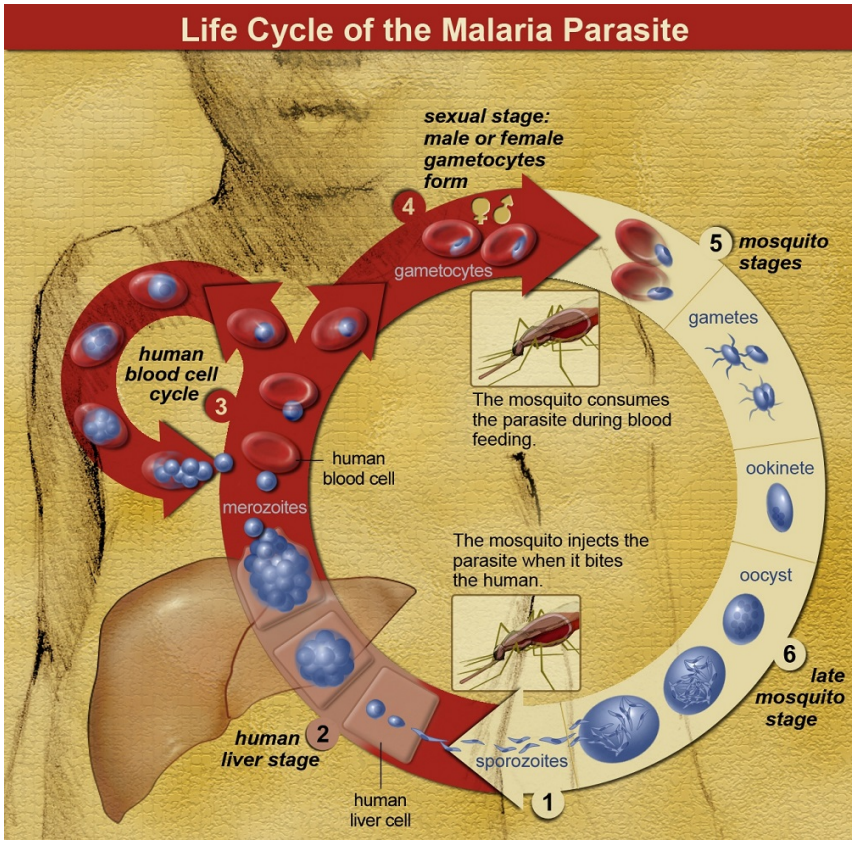

Figure 1.3: Lifecycle of malaria parasite: After mosquito bite, the sporozoites of *plasmodium* gets in blood circulation till the liver where it starts schizogony. After that, merozoites are released in blood circulation. They will attack erythrocytes and the cycle is closed when a mosquito bites and gets both the gametocytes [21].

1.2 Approach

Following the above outlined needs for each case study, EIS technique emerges. The main objective of this dissertation is to present the full potential associated with the use of impedance spectroscopy, particularly in terms of detection of contaminants in the waters at the exit of the treatment plant, in moisture detection in PET flakes right before the melting and in malaria parasite uncovering in human blood.

This method distinguishes easily, and with relative good sensitivity, changes in physical and chemical composition of fluids and materials under study, which makes it a potential detection technique for specific changes in every case study presented. Since the water study is the most cited case, all the methods started with water tests.

This device is simple to use on a bench and easy to adapt to the groundwork. It is relatively cheap when compared with the currently performed tests for each case (especially

when laboratory tests are discussed). It is a rapid technique (takes about 30 minutes) and it is portable. It is robust and it deserves a thorough investigation of possible new applications.

1.3 System Requirements and Constrains

The major request of actual industry is to find the easiest way to detect problems. When easy and cheap must come together, other characteristics (such as material used and its durability, the time of use, among others) must be suppressed despite being always considered.

During the studies presented some requirements were considered in order to turn the device cheaper and accurate at the same time. Respecting the final applications for each case study, the most accurate and cheap electrodes were selected as presented ahead.

Although known, the requirements for electrode durability when exposed to such aggressive environments, it has been taken into account whether the sample should be reused or must be discarded after the test. All electrolyte physical and chemical changes brought were studied and considered.

For the water contamination and malaria disease tests, stainless steel wires are used to manufacture the electrodes, since this is the most resilient and cheap material. The water and blood samples are used just once since the sample holder is disposable. The sample holder volume was minimized in order to fit the device and the blood collection requirements.

In the case of PET moisture stainless steel electrodes are also used. The electrodes for PET must have a higher area in order to create a higher intensity of the electric flow. The material was the most resistant to corrosion and erosion during testing. The PET environment is less aggressive than the previous ones, thus some cleaning specifications are required only. The shelf life of those is under study. These characteristics are still being optimized.

Chapter 2

State of the Art

This chapter will present the latest works and most relevant research in the area of study here investigated. For each case study, features and methods are presented for the existing and currently most used devices. A common trait is transverse to the 3 case studies: with the proper functioning of the device under study, the lack of portability, high price and the difficulty of handling are overcame faults.

2.1 Case Study 1 - Water Contamination

A water treatment plant needs to ensure that no contaminants goes out the circuit and gets into water cycle. For that, microbiological, physical and chemical tests must be performed.

It is preferred to get analytical methods to distinguish multi-waste and not only metal ions and antibiotics.

Thus the fluorescence spectroscopy is the gold standard to detect water contaminants. This technique is based in excitation-emission matrices (EEM) and synchronous fluorescent spectra (SFS) [25]. EEM works by fluorescence maps based on emission scans acquisitions for a wavelength excitation range and SFS uses simultaneous scanning of the excitation and emission for a fixed wavelength range. However, fluorescence spectroscopy requires high performance equipment which turns the process highly expensive.

The presence of specific antibiotics and metal ions, which showed the most persistent contaminants in the environment, is currently studied by ultra-high-performance liquid

chromatography (UHPLC) or tandem mass spectrometry [26].

The purpose of the device under study is to increase the range of contaminants covered and to distinguish the various components making it easier to analyse, without requiring laboratory tests, reducing costs in many ways.

2.2 Case Study 2 - PET Moisture

Once PSW production is growing every year during past decades, also recycling processes optimization techniques were deeply studied [12]. One of the most problematic steps in recycling PET is the moisture detection for dry process, before the moulding. Thus, this will be the object of study hereafter.

One of the more often used hygrometer in industrial levels is the MEECO - an electrolytic system connected to a heating system. Air enters in the system and runs through a series of electrodes that lie inversely polarized as shown in Figure 2.1.

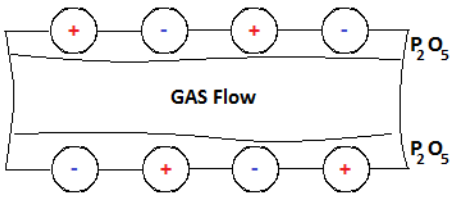

Figure 2.1: Representation of the electrolytic cell. When the air passes through the electrodes, it electrolysis each water molecule receiving two more electrons in the cathode [27].

Each molecule of water gives two electrons between the anode and the cathode, forming a current electrolysis - that allows us to calculate the amount of water molecules entering the cell.

This technique allows the calculation of the moisture concentration in the gas [27]. It is used to extrapolate the air moisture. This is a conductance study technique as EIS.

Some other studies using EIS were performed lately. The use of conductance properties is attractive due to its wide range of physical properties [28–30].

The device under study respects the EIS technique. However this study is based on non-treated surface electrodes in order to get the lowest price.

Following the information given by a highly regarded plastic containers producer (LOGOPLASTE), the most fast and cheap method of moisture detection in PET is the accurate weighing of the provided sample and its density study in comparison with a dry sample.

Duration of PET's drying process is only optimized by varying driers area, temperature and isolation, never taking into account how wet PET is. This study must find a better way to quantify the moisture rate to optimize the time and temperature of drying.

2.3 Case Study 3 - Malaria Disease

Traditional malaria diagnosis techniques are based in laboratory and molecular analysis. At the forefront of laboratory diagnostic tests are microscopy based techniques, like Peripheral Blood Smear (PBS) or DNA inspection and RDT's. Molecular tests are also used. Polymerase Chain Reaction (PCR) and Microarrays techniques are the most used and developed [19].

During the last decade, malaria diagnosis methods suffered a fast and positive development. However, the high price associated and the high level of skills required to use the most accurate diagnostic methods, make them not suitable to be used in underdeveloped countries.

Previously, studies were performed to distinguish blood characteristics based on the fluid conductance [22]. The method is different from the one presented in this thesis since gold surface changed electrodes are used. The method uses low frequency to study the cell circulant environment. The blood needs previous treatment in order to separate erythrocytes. A Voltalab 80 PGZ 402 is used for data acquisition. Another method used micro-flow cytometry combined with EIS analysis and it reveals cell impedance changes when parasitized. [31]. In order to turn this test non-invasive, some studies in magneto-optical properties are in progress [16, 32, 33].

Since EIS fits the requirements for malaria screening, the aim of this project is to develop a portable, easy to use and accurate system, that presents also high sensibility to hemozoin detection. The device under study during this thesis is relatively cheap and easily replicated. It has been earlier studied by Paula [34] concluding the possibility of

application of the EIS technique, although using different device components and materials. Paula's device uses hardly portable and expensive electronic equipments and also treated electrodes, which turns the method more expensive than ours.

Chapter 3

Theoretical Background

In this chapter the main technique used is described. The screening and measurement of contaminants in water, moisture in PET and malaria parasite in blood full-blown over the current work is based on EIS. To this equipment, a magnetic field provided by an Halbach cylinder, for malaria tests, will be attached. The theory behind the method is slightly explained henceforth.

3.1 Electrical Impedance Spectroscopy

The impedance is the property that describes the opposition which a material offers to the flow or an electric current with a given frequency, in a system [35, 36].

Impedance is often simplified as a result of input voltage division (V-Volts) by input current (I-Amperes) as:

$$Z^*(\omega) = \frac{V_0}{I}\sin(\omega t - \measuredangle Z^*) \tag{3.1}$$

where ω is the angular frequency, $\omega = 2\pi f$. The potential differences are responsible for the current flow appearance and by the movement of the electric charges for the benefit of the gradient. Current explains electrical charges flow per time [35]. EIS technique is based in the excitation of a sample by an electric field with a varying frequency. The two impedance important relations to refer are amplitude, $|Z^*|$, and phase, $\measuredangle Z^*$. This last translates the angular phase shift through which the current delays from the voltage.

Amplitude is given by:

$$|Z^*| = \sqrt{(Re\{Z^*\})^2 + (Im\{Z^*\})^2} \tag{3.2}$$

and the phase is given by:

$$\measuredangle Z^* = \arctan \frac{Im\{Z^*\}}{Re\{Z^*\}} \tag{3.3}$$

Impedance may be represented by two components: the real part of impedance, $Re\{Z\}$, which is the **resistance** – dissipated energy – and the imaginary part, $Im\{Z\}$, which is the **reactance** – stored energy – and they are given by:

$$Re\{Z^*\} = |Z^*| \cos \measuredangle Z^* \tag{3.4}$$

$$Im\{Z^*\} = |Z^*| \sin \measuredangle Z^* \tag{3.5}$$

Direct Current (DC) measurements only provide the value of the total conductivity, and do not return information about the different contributions of conduction mechanisms that can occur in certain materials. Through EIS method it gets possible to obtain additional information such as dielectric polarization and driving mechanisms. This information would not be detected by simple measures of conductivity in DC since it can only have the real component information.

EIS is nowadays used in a wide range of applications such as cellular measurements (counter, hematocrit measurements, cell culture monitoring, among others), volume changes measurements (in cardiography, plethismography and pneumography), body composition (water, fat, among others), tissue classification among others [37, 38].

3.1.1 Measurement Principles

An 1V sine wave is introduced by the wave generator in impedance meter system. The test object can be excited by a current (MI), when the sample is positioned in the operational amplifier feedback path, or by a voltage (MV). The circuits for representation of these two modes are presented in Figure 3.1.

An inverter configuration is used. Consequently for each current and voltage modes

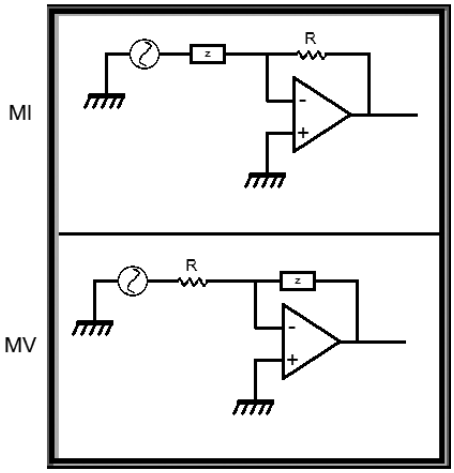

Figure 3.1: Excitation modes schematic: Here are represented the inverter simplified circuits for current mode (MI) and voltage mode (MV).

and for inverter configuration, the signal expected to obtain is for current mode (MI):

$$V_{out} = -V_{in} \times \frac{Z}{R} \tag{3.6}$$

with gain $\frac{Z}{R}$, and for voltage mode (MV):

$$V_{out} = -V_{in} \times \frac{R}{Z} \tag{3.7}$$

with gain $\frac{R}{Z}$.

In these equations, Z represents the object under study (load between the electrodes) and the R represents the internal equivalent resistance. The **-** signal explains the inverter input. In the oscilloscope two signals (input and output) have to be in phase opposition.

The frequencies were chosen in order to get an output signal:

$$0.2 < |V_{out}| < 5 \tag{3.8}$$

Output signal saturation occurs for $|V_{out}| \geq 15V$. Thus the calculus of the gain is crucial in order to define which is the best resistive element.

In order to study the presence of conduction processes for simple tests, Cole-Cole plots are drawn. In this plots resistance is in the x-axis and the symmetric of reactance ($\times -1$)

in the y-axis. For more complex studies other important representations to use are $|Z^*|$ V_s $\log(f)$ and $\measuredangle Z^*$ V_s $\log(f)$. The $\measuredangle Z^*$ is the value of phase shift angle [39].

Taking into account moving charges present, four main physical processes may have influence on data:

- bulk resistive-capacitive and generation-recombination effects;
- adsorption at the electrodes;
- electrode material reactions;
- diffusion.

It is important to take into account parasitic impedances which can defect the results. These impedances are neglected when electrodes area is large (more than $1cm^2$) and the frequency ranges above $10kHz$ [39].

3.1.2 Equivalent Circuits

Some equivalent circuits are in consideration in order to develop the most accurate and simple impedance meter. In the Table 3.1 some circuits and the characteristics that make them considerable are listed. This circuits were used in previous studies in which the importance of impedance data acquisition in several material properties interpretation were demonstrated.

The impedance meters interpret RLC circuits. These circuits enable the absence of reactance reference values, since this is readily calculated by knowing the excitation signal frequency, current and voltage. It is noted that impedance meter bridges allows a versatile design for various applications [40].

The first two are considered by Feucht [40] the core of the impedance measurement circuits. The first one presents a load virtual ground as the one presented in 3^{rd} and 4^{th} raw, which are the ones used in the present case studies, for MI and MV, respectively. The second one has the Load Z_x grounded.

Table 3.1: Equivalent Circuits for inverter mode from literature [40].R_g is the internal resistance, ahead represented by R_{int}. V_{Vx} translates the amplified voltage and V_{Vi} results from the $V_{Vi} = i \times R_g$, with i as the source current.

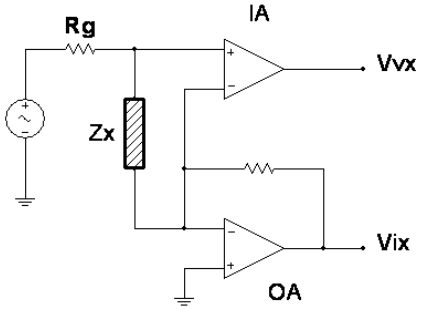	Load virtual ground
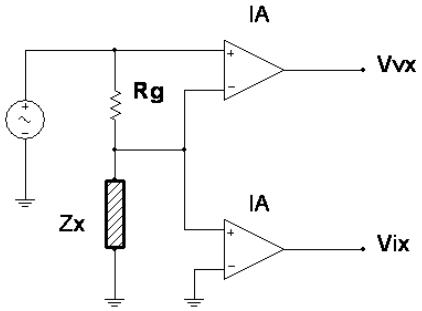	Grounded Zx
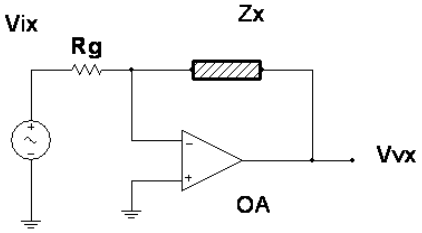	Load virtual ground
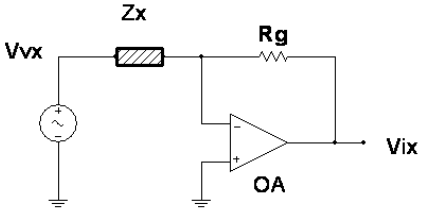	Load virtual ground
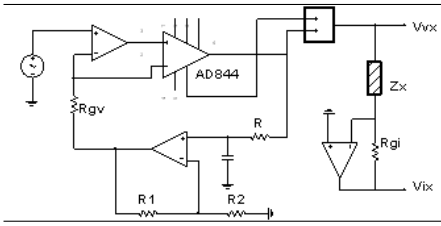	Zx - virtual ground Current feedback OpAmp (AD844) Load virtual ground

3.2 Halbach Magnetic Field

Magnetic fields are sourced mainly by the existence of permanent magnets in proximity. Its field lines have specific properties. They are represented by force lines, which indicate at each point the direction (tangent to the force lines) and direction of the magnetic field. They leave the north pole and enter the south pole, continuing within the magnet in the direction of north pole, forming closed lines as illustrated in Figure 3.2 [41].

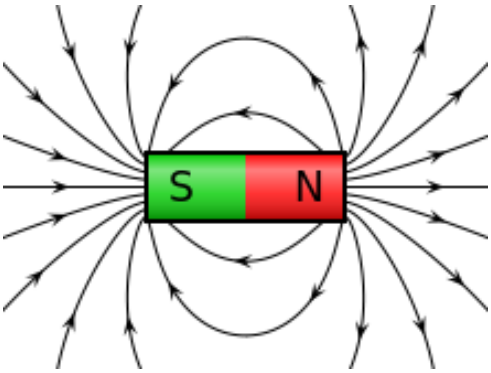

Figure 3.2: Magnetic field force lines of an ideal parallelepiped magnet [42].

A magnetic field can also be created by the inductive movement of charges - electric field. In this case force lines are circumferences, and the field strength depends on the distance to the current. The direction of the magnetic field is thus given by the right hand rule.

Ampere cited *"The line integral of a magnetic field at any closed curve is proportional to the amount of electric current in all the conductors which cross the inside of the curve"* translated in:

$$\oint_C \overrightarrow{B} d\overrightarrow{r} = 4\pi k_m I_{int} \tag{3.9}$$

where $k_m = \frac{\mu}{4\pi}$, I_{int} is the total current of all conductors and the μ is the permeability, a material dependent parameter. This equation allows us to calculate the magnetic field value when generated by an almost infinite electrical string.

Once a continuous magnetic field is required for malaria detection tests, the magnetic cylinder Halbach was resorted. Halbach exposed ideal models of continuous magnetization, even being so hard to fabricate.

Some authors have studied the magnetic field changes by different configuration of

Figure 3.3: Magnets horizontal polarization.

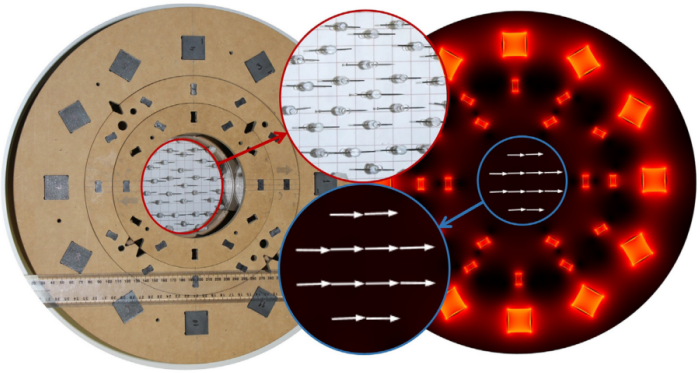

Figure 3.4: Continuous magnetic field generated by Halbach 12 magnets as reported by Vogel [43].

permanent magnets in order to get the best Halbach configuration [43–46].

This way a set of 12 magnets with horizontal polarization (as shown in Figure 3.3) are disposed in a cylinder with 60 degrees rotation from each other getting a configuration as presented by Vogel [43] in Figure 3.4.

3.2.1 Crystals Alignment

The Halbach cylinder will be used to magnetize hemozoin pigments in malaria diagnosis. Hemozoin is a changed hemoglobin which acquired ferromagnetic properties. It is a pointed shape crystal as shown in Figure 3.5(c) which is capable of aligning itself in the presence of a magnetic field [16]. As shown in Figure 3.5(b), hemozoin molecule has a central magnetization axis containing ferritic ion. This molecule has an arrangement as shown in Figure 3.5(a).

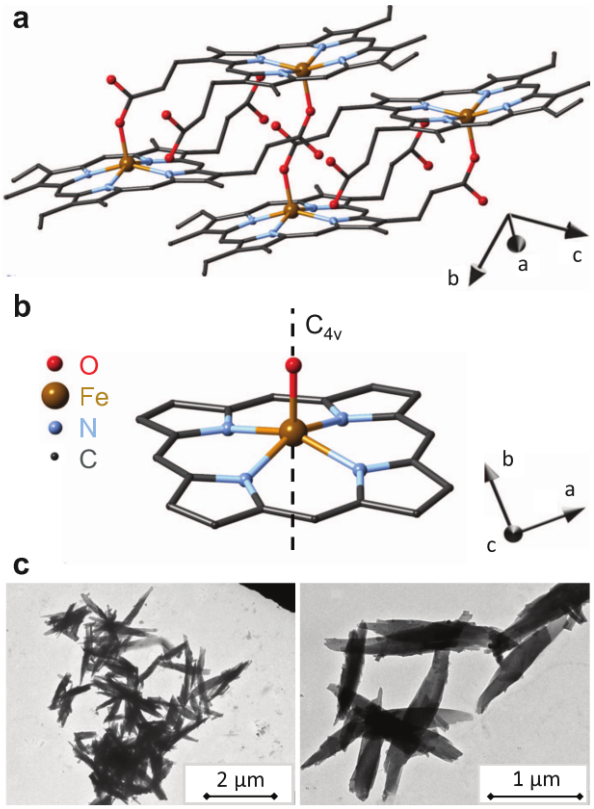

Figure 3.5: Hemozoin structure which gives it ferromagnetic properties: *(a)* is represented in its molecular structure; *(b)* is the atomic arrangement that evidences the axis of magnetization; *(c)* the microscopic Capture of hemozoin highlighting its pointed shape [16].

Chapter 4

Materials and Methods

The materials of study and the methods used to achieve the main goal will be summarized in this section. Both the materials and the methods were defined having in mind the achievement of accurate component distinction in the three cases. In the first section the materials used will be minutely described, starting with the Hardware, then the Software followed by the Tools and the Test Objects. The second section will contain the methods developed. Since three cases are studied, a detailed description of each case will be provided.

4.1 Materials

4.1.1 Hardware

The hardware, resumed in Figure 4.1, is composed by a power supply system,a wave generator (Digilent®) which is controlled by $MATLAB$®, a motor driver to control the motor responsible for Halbach cylinder rotation, an impedance meter circuit, a thermometer based in a thermal resistor (PT1000) and the electrodes which are embedded in the sample holder. A buffer circuit is added for PET tests. For acquisitions in hostile environments, the system is placed in a Faraday cage.

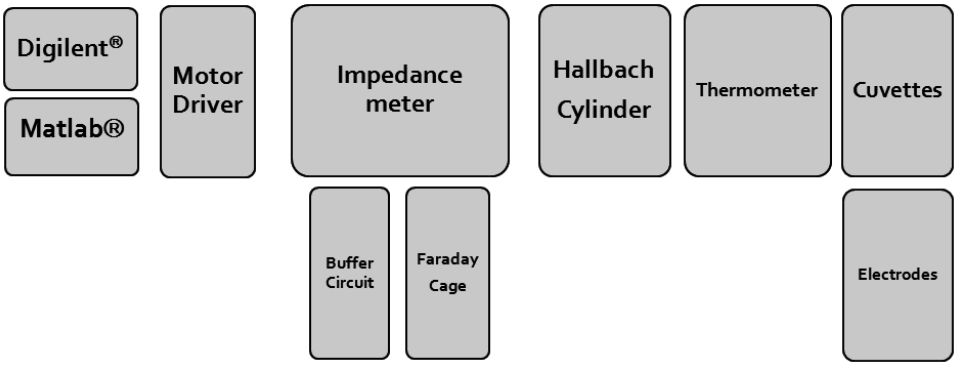

Figure 4.1: Hardware Architecture resume.

Power supply

At the moment the system is powered by 220V AC. This voltage is converted to $+12V$ DC which will supply the 12V motor and its driver. These $+12V$ are converted to $\pm 15V$ DC and $\pm 5V$ DC in order to supply impedance meter amplifier and the thermometer respectively. Internal components like LEDs and switches are fed by $+5V$ DC.

Digilent® Analog Discovery

The Digilent® Analog Discovery system from *Analog Devices Inc.* is able to measure, record, and generate analogue and digital signals. The device is represented in Figure 4.2 [47]. It is a multi-function device which replaces several electronic instruments simplifying data acquisition. Its most important features for this study are:

- 2 simultaneous acquisition channels;
- Sampling up to 100 MS/s;
- 5VDC power supplies
- Easy interface with matlab - toolbox for Digilent.

In addition to these features, it is still small, lightweight, inexpensive and portable, requiring a low power supply.

Motor driver

A stepper motor is used to rotate Halbach cylinder for precise angles. This motor type is Y129 and it is able to rotate with high precision 200 steps of 1,8 degrees [48].

Figure 4.2: Digilent® Analog Discovery system from Analog Devices Inc.

Impedance Meter

Once studying the impedance inherent in a circuit, it becomes necessary to use a reliable and precise instrument for the impedance measurement. Thus one impedance meter based on voltage and current deflection measures was built. This instrument is connected to the Digilent® which allows to acquire the signal resulting from the excitation circuit by a DC voltage of $\pm 15V$. Its general circuit is represented in Figure 4.3.

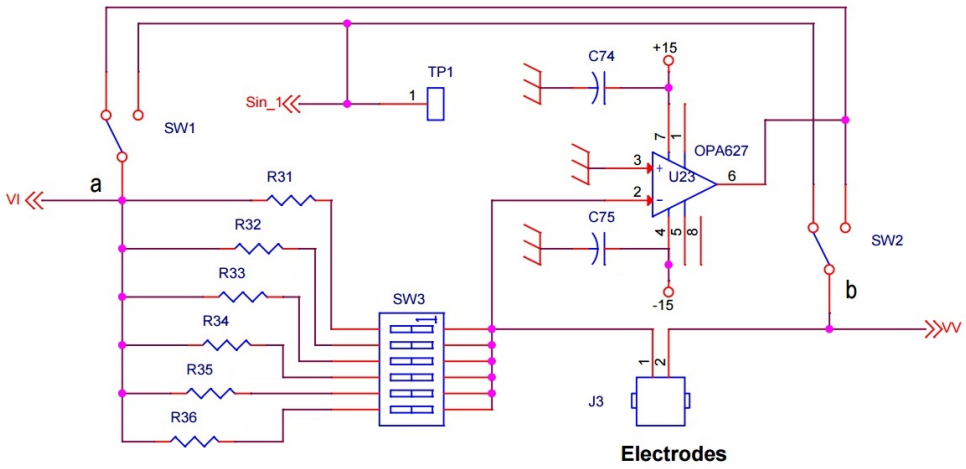

Figure 4.3: The impedance meter circuit is represented in order to understand the acquisition mechanisms. It allows to switch channels in order to change the internal resistance of the circuit and the excitation mode (current - I or voltage - V).

The internal circuit is organized in order to change 2 parameters through the deep switches: internal equivalent resistance and voltage/current mode.

(a) Up view

(b) Up View

(c) Up view circuit

Figure 4.4: The first version of the impedance meter in (a) was a simple circuit with an interrupter and a mode switch button. There is a whole which allows internal resistance change. The second impedance meter in (b) and (c) allows inverter and non-inverter mode switch.

Various circuits have been used to study different possible ways to characterize these materials and fluids. The first two impedance meter used are represented in Figure 4.4. Once inverter and non-inverter configurations were studied, a second device was designed to cover those needs. Thus impedance meter 2 was assembled as shown in Figure 4.4(c). The second impedance meter allows to switch between inverter and non-inverter mode and also between current and voltage modes. Such as the first device it has a whole to allow internal resistance change.

It was found the inverter mode is the most reliable mode for the objects of study, so the Impedance meter 2 was only for the first experiments. This system respects the base circuit represented in Figure 4.3. This way, the most accurate printed circuit board was designed and it is represented Figure 4.5. The board is ready to receive two distinct systems. In this case, we will focus in impedance measurement system.

The PCB revealed to be more accurate and less sensitive to errors. This last device was used to obtain the most accurate results for each case study. The 3D printed structure in PLA is adaptable and changeable for each case - for PET analysis, a copper coil – buffer circuit – is added and for malaria analysis an Halbach cylinder is attached.

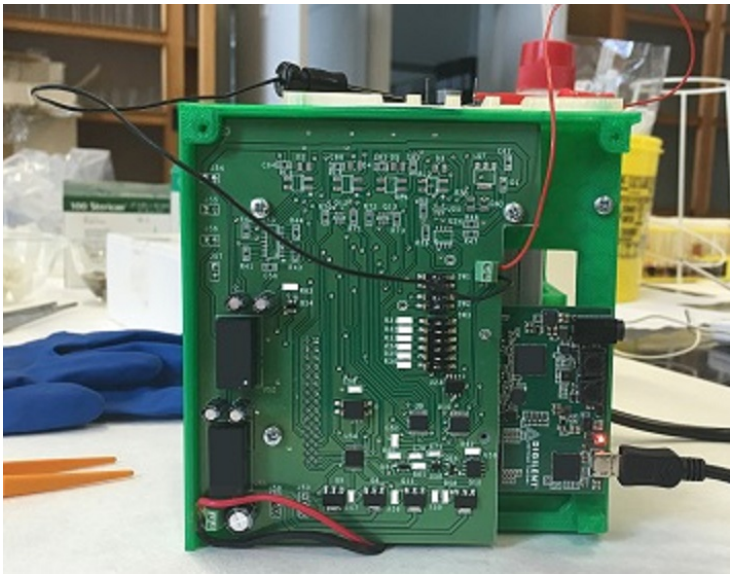

Figure 4.5: The third impedance meter was printed PCB with several deep switches which allows to change parameters easily and with less human mistakes or verification needs.

Halbach cylinder

In order to generate a uniform magnetic field, important to ferromagnetic pigments detection, we appealed to the Halbach configuration of magnets. In this configuration, permanent magnets are used in the formation of a cylinder. This cylinder has an intense magnetic field inside without magnetic field outside as represented in the Figure 4.6. The

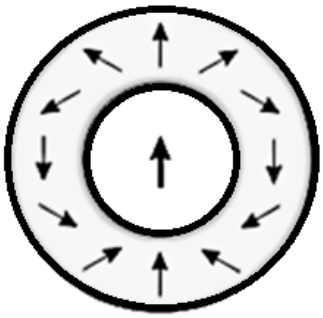

Figure 4.6: The magnets configuration forms a nearly uniform magnetic field in the center of the cylinder.

Halbach cylinder used is an assembly of twelve permanent magnets. The magnetic field generated inside this cylinder has $\frac{1}{3}T$ right in the centre of the whole. This component will be used for malaria tests.

Temperature Sensor

Due to the high influence of temperature in impedance results, a thermometer was tested in order to be added to the system in the future allowing to normalize the impedance measure taking into account its variation with the temperature. This thermometer has a temperature sensitive resistance PT1000. Its circuit is represented in Figure 4.7. Some tests were performed and presented in the Chapter 5 in order to ensure thermometer linearity and sensitivity. PT1000 data-sheet information was used to extrapolate the temperature value through V_{out} values [49]. Resistance variation is obtained by:

$$R_T = \frac{V_{out}}{\frac{\Delta V}{1000} \times (1 + \frac{R_{62}}{R_{61} \times (R_{62}\omega C + 1)})} \tag{4.1}$$

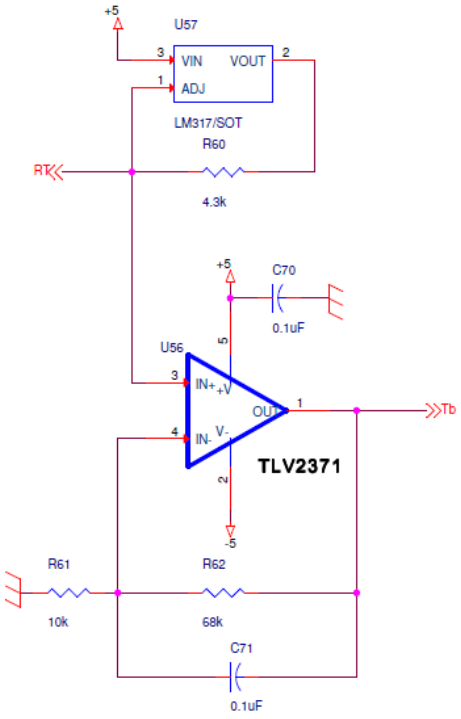

Figure 4.7: PT1000 circuit. The thermal resistance is represented by RT.

Sample holders

The test object holders were composed by a cuvette of polystirene (PS) for the water and blood studies. All the electrode support structures are 3D printed pieces of Polylactic acid

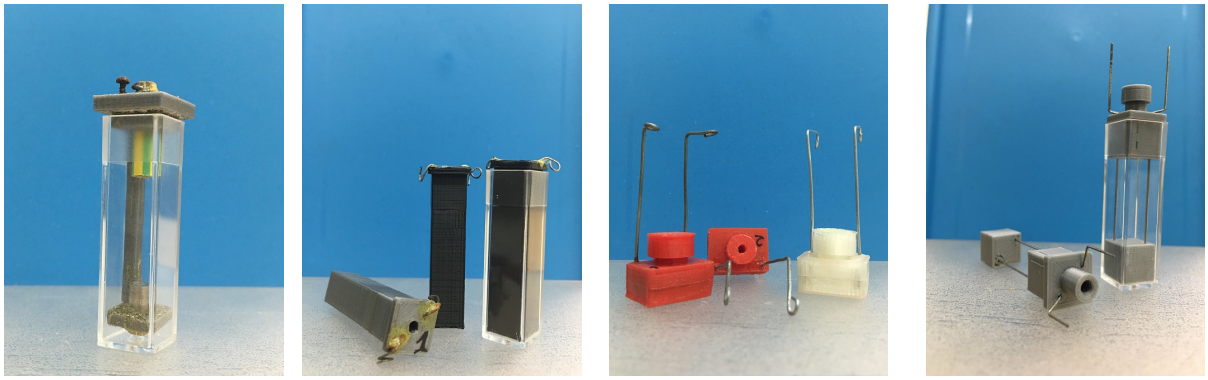

(a) Cuvette 1 (b) Cuvette 2 (c) Cuvette 3 (d) Cuvette 4

Figure 4.8: The container 3 is an attempt to minimize the volume of tested material. Some constraints with the fluid placement occurred. The cuvette 4 is the last version used in water and blood samples.

(PLA). The electrodes used are made of stainless steel. The minimum volume is required to blood sample tests since the intention is to use the least amount of blood as possible, making the method less intrusive. The four containers used are represented in Figure 4.8. The cuvette 1, Figure 4.8(a) was composed following the water tests results in a water trough. In order to have a minimum volume sample, cuvette 2, Figure 4.8(b) was tested. Its volume was five times smaller than the cuvette 1 volume. After realizing the electric field was not aligned with the magnetic field, which was important for malaria detection tests, the container was drastically changed to cuvette 3, Figure 4.8(c). This shape allows low volume requirements. However the container is completely matted which does not allow to view the contents of the cuvette, not allowing for checking of the existence of air bubbles or other artefacts that may change the results. Thus cuvette 4, Figure 4.8(d), was built to fill those gaps. The structure combines all previous requirements - we can get a lower volume and it is possible to inspect cuvette interior during data acquisition. The sample holder configuration is crucial to the proper placement of the sample.

The associated cost corresponds to the needs of a disposable container. The material used is biocompatible which is indispensable specially to blood tests. The container was optimized in order to achieve a suitable volume sample required.

Electrodes

The electrodes used to study fluid and material characteristics were based in stainless steel material. This material is cheap and allows the disposability of the container after electrolyte study. The stainless steel used for first water tests was those presented below and shown in Figure 4.9.

Figure 4.9: First electrodes used to water tests: YT 10,9, ZP 8,8, A4 80, A4 70, A2 70, respectively.

The first two materials are zinced steel coated with a carbon alloy and zinc. The A4 and A2 are based in a Ni-Cr alloy with different proportions (10-14% Ni + 16-18.5% Cr for the first case and 8-13% Ni + 17-20% Cr for the second case). A4 electrodes revealed to be the most corrosion resistant as expected. The numbers after the type represents the tensile strength divided by 10 (for example, A4 80 has a tensile strength of $800N/mm^2$). The electrodes were partially isolated to maintain constant the contact area. Different colours were used to facilitate material distinction.

Electrodes evolute to shorter forms in order to get smaller sample holders. This way, for water and blood tests, stainless steel wire was used. The wire has a shorter area which will increase impedance value – this is crucial since commercial waters and blood samples are very ionic, having very low impedance, which saturates the system.

Specially for PET impedance measurement, electrodes evolutes from stainless steel rods ($radius = 0.4cm$ and $length = 25cm$ separated by $0.5cm$) to steel plates ($width = 12cm$ and $length = 25cm$ separated by $0.7cm$) as presented in Figures 4.10(a) and 4.10(b), respectively.

Buffer Circuit

Since PET changes its behaviour with frequency changes, behaving as open loop for the low frequencies and as a short circuit for high frequencies, it was introduced in the system a circuit as presented in Figure 4.11(a) with a resistance in series and a coil in parallel

(a) Rods $25cm$

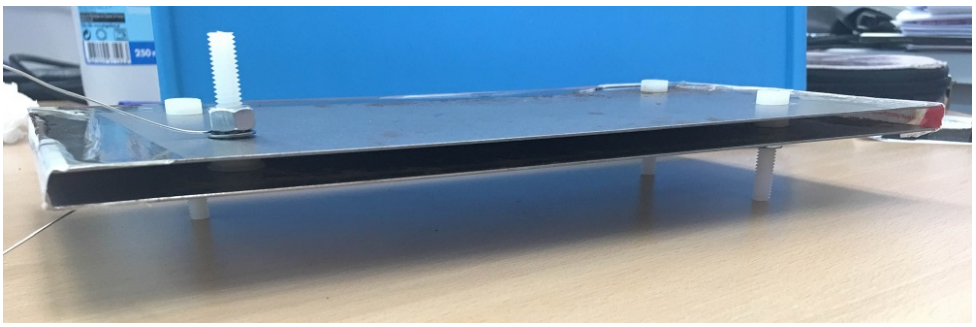

(b) Plate $25 \times 12cm^2$

Figure 4.10: PET electrodes shapes. At first, stainless steel rods were used and finally it was changed for stainless steel plates.

as represented in Figure 4.11(b). The resistance eliminates the short circuit and the coil eliminates the infinite impedance which results in open loop.

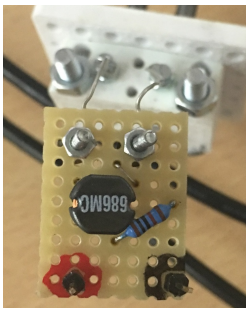

(a) Buffer Circuit and schematic.

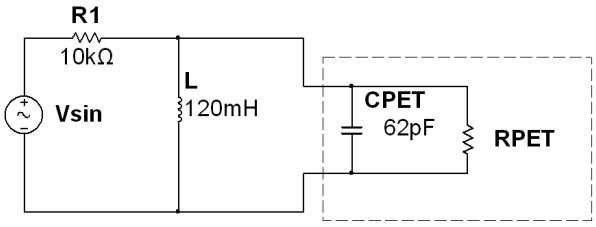

(b) Buffer Schematic.

Faraday Cage

A Faraday Cage is a shield formed from conductive materials. It is a wrapper normally comprises a conductive loop connected to ground. This cage blocks static and non-static fields, protecting the inside of electromagnetic interactions. It does so through channelling

the power over and around, but not through the interior. The conductive material delivers constant tension from all sides of the casing. The cage is represented in Figure 4.11.

Figure 4.11: Faraday Cage.

This cage is used for acquisitions in hostile environments to filter the interferences from outside the system that affect the acquired signal and introduces noise in output signal.

4.1.2 Software

The Digilent® requires a software development kit (SDK) previously installed in the computer to permit data exchange. The SDK is available on the website [50].

The whole project was developed using *MATLAB® R2015b*. There were developed the data acquisition files to communicate with the device. The user can control the device through an interface as represented in Figure 4.12. All the impedance parameters related to wave generated parameters and to the impedance mode and magnetic fiend rotation mode can be controlled through the black box. In the red box it is possible to shut on/off the acquisition system, choose the direction of magnetic field rotation and it's rotating parameters. In the yellow box data type is set. For impedance case it is possible to choose Impedance slot. For temperature tests it is the only check point required. In green box internal resistors are chosen. Angle of rotation or number of steps can be selected in the purple box. It is possible to choose the Single Frequency or Standard Sweep, with the option of repeat the single, in the orange box. If repeat single slot is chosen, it is possible to select time between repetitions and how many times to repeat in blue box. The colours

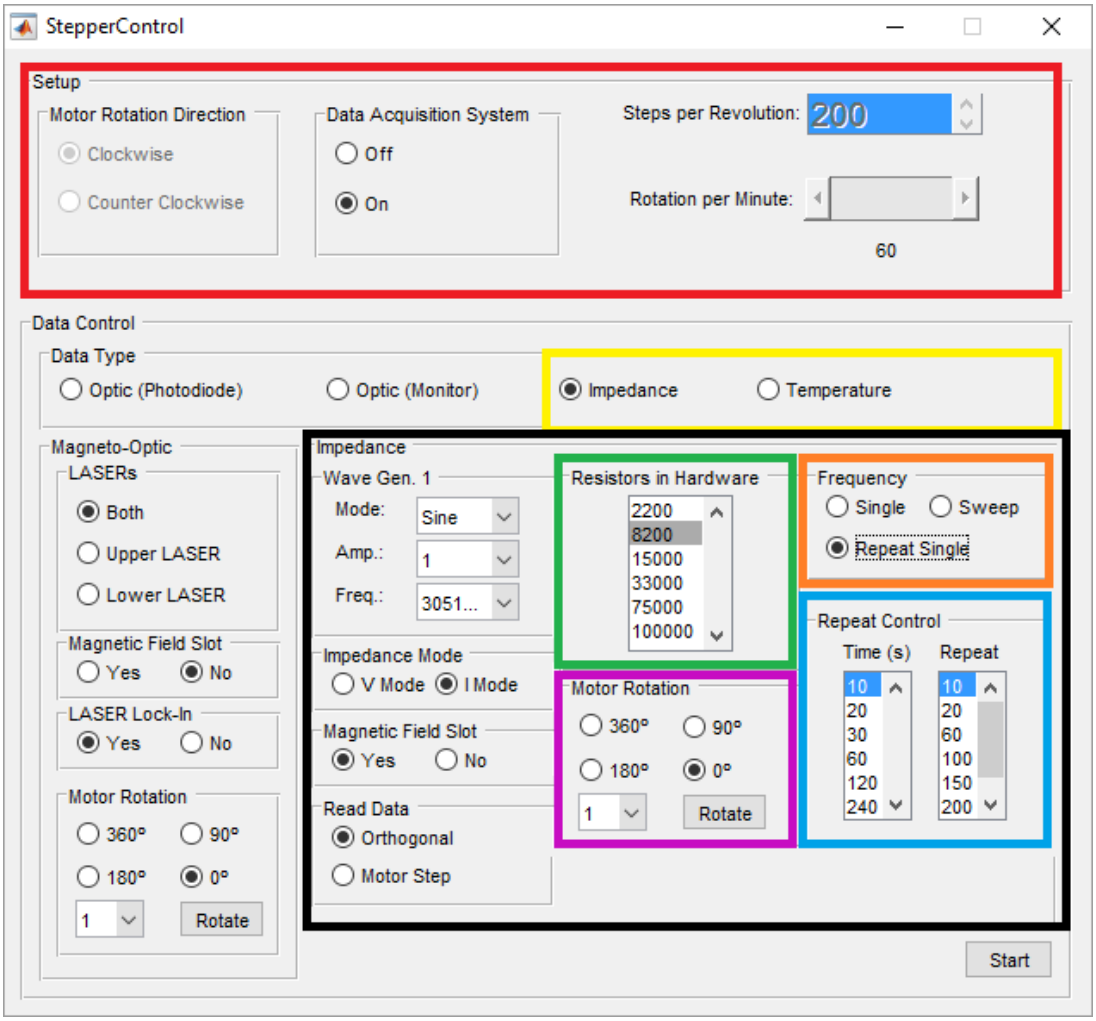

Figure 4.12: MATLAB® interface.

presented are merely representative in order to explain where the parameters are selected or changed.

4.1.3 Tools

Some tools have been used to measure external parameters namely:

- Thermometer (*SIKA*® and *CATIM*®);
- ATPK2 PEAK®(semiconductor component analyser);
- *MATLAB*® *R2015b* academic licence from The MathWorks, Inc.

Table 4.1: Composition of the waters under study

	Penacova	**Vitalis**	**Luso**	**Vimeiro Lisa**	**Fastio**	**Vimeiro Original**	**Caramulo**	**Evian**
pH	5,3 (0,4)	4,7	5,8 (0,2)	5,88 (0,4)*	6 **	7,3 (0,2)*	6,5	7,2
Total Mineralization	32 (2)	26	48 (7)	48(5)	-	1035(30)	86	-
Total Hardness	-	-	8,8 (0,7)	-	-	-	-	-
Dried Residue	-	-	42 (4)	-	34 (4)	-	-	309
SiO2	8,9 (0,4)	10	13 (2)	0,6(0,1)	9,6 (2)	13,1(0,6)	28	-
Anions								
Cl-	9,9 (0,4)	7,2	9,1 (0,5)	10(1)	4,2 (0,4)	198(16)	5,2	6,8
HCO3-	2,3 (0,5)	<0,3	12 (4)	16,8(0,5)	8(0,8)	448(5)	26,6	360
SO4 2-	1,3 (0,2)	-	1,5 (0,2)	-	1 (0,2)	-	-	12,6
F-	-	-	-	<0,1	-	0,29(0,01)	-	-
NO3 -	1,9 (0,2)	1,3	1,6 (0,2)	-	-	-	1	3,7
Cations								
Na +	5,3 (0,4)	4,2	7,1 (1,1)	9,5(2)	4,1 (0,4)	139(14)	11,3	6,5
Mg2+	1,1 (0,2)	0,7	1,7 (0,2)	1,4(0,5)	-	30 (2)	1,7	26
Ca2+	0,5 (0,1)	0,4	0,74 (0,12)	5(1)	1,3 (0,3)	119(9)	2,7	80

mg/ml *20° **18°

4.1.4 Test Objects

Waters

Attending to our objectives of distinguish water components, several waters from different sources were used. The labelled composition of them is represented in Table 4.1. Deionized water and distilled water were also used to software calibration.

PET

The PET used to simulate the influence of environmental moisture came from two different providers as shown in Figure 4.13. Therefore, it is considered important to ensure that the shape of the pellets (Figures 4.13(a) as cylinders and 4.13(b) as spheres) will not affect the results to the concentration of water and moisture.

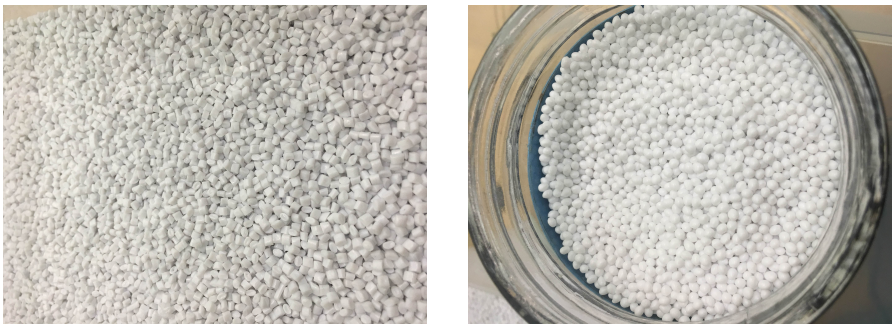

(a) PET 1 (b) PET 2

Figure 4.13: The PET received presented two different shapes as shown above (4.13(a) cylinders and 4.13(b) spheres).

Blood

In order to get closer to the circumstances of detecting malaria, two types of blood were used. Firstly rabbit blood with synthetic hemozoin and then human blood. Rabbit blood was provided by *Probiológica* and it is preserved with the anticoagulant *acetyl-CoA carboxylase*. It was diluted with *Sigma* PBS (Phosphate Buffered Saline) P4417 with $pH = 7,2$ in the proportions described in Table 4.2 [51].

Human blood was 50% diluted with PBS with $pH = 7$ whose composition was: distilled water ($2l$); potassium chloride ($400mg$); Sodium chloride ($16mg$); potassium dihydrogen phosphate ($400mg$); sodium dihydrogen phosphate ($2.3g$); phosphoric acid 8.5%. This

Table 4.2: Dilutions of the blood used for the three tests with the containers Wire 1,2 and 3 and for excitation in MI and MV. The dilutions are presented in PBS:Blood proportion. With Synthetic hemozoin (HzS) the dilution is related to HzS:(blood:PBS (1:1)).

	MI		**MV**	
	No HzS	**With HzS**	**No HzS**	**With HzS**
Wire 1	1:1 1:2 1:4 1:8		1:1 1:2 1:4 1:8	
Wire 2	1:1	10:1 20:1	1:1	10:1 20:1
Wire 3	1:1	3:1 20:1	1:1	3:1 20:1

Table 4.3: Human blood samples were provided by the National Institute of Forensic Medicine and Forensic Science (INML.CF), Delegation of Centre.

Sample	**Origin**	**Age**	**genre**
1	Madeira	30	Male
2	Madeira	39	Male
3	Madeira	59	Male
4	Madeira	64	Female
5	Madeira	56	Female
6	Center	20	Male
7	Madeira	42	Male
8	Center	52	Female
9	Center	62	Male
10	Center	65	Male

blood was treated previously with a buffer of Potassium Fluoride (Na_2EDTA). The samples used are described in Table 4.3.

Synthetic Hemozoin

Synthetic Hemozoin (HzS) was used to simulate the presence of malaria in blood samples. HzS used was manufactured in laboratory.

4.2 Methods

Two methodologies were in the base of this study. The **Standard Sweep** and the **Single Frequency** tests. Both the methodologies are always tested in the voltage and current modes, here referred as MV and MI respectively.

Deep switches are in the circuit in order to select internal equivalent resistance or to select excitation mode (voltage or current mode) varying or not the frequency. Some tests were performed to understand, if inverter or non-inverter mode was the better. The device used presented an inverter configuration. It is expected to obtain, for each mode MI and MV, a reverse result taking into account the charge flow between the electrodes and the internal resistance in the system. The MI and MV results for inverter mode will be presented hereafter.

All the studies start with a Standard Sweep in order to visualize which is the best frequency to use in Single Frequency repetitions. After the circuit understanding it is important to explain the main acquisition methods.

For each method three graphics are generated:

- $|Z|$ (presented in Ω);
- $\measuredangle Z$ (presented in degrees);
- Cole-Cole diagram.

4.2.1 Standard Sweep

Sweep standard uses a frequency list (from $1Hz$ up to $1MHz$) and calculates impedance modulus, phase and Cole-Cole Diagram for each frequency. Cole-Cole Diagram is used, in this case, to understand the ability of the material to conduct electric current.

4.2.2 Single Frequency

The best frequency is selected by observing the output signal (output signal framed between a minimum measurable signal and a threshold before signal saturation). This is observed by performing a sweep study. This test allows us to study variation of conductance

with time, keeping constant the external parameters which influence the measurement (eg. temperature).

Case Study 1 - Water Contamination

Water impedance spectrum is studied in this case. The special attention is given to resistance and reactance variations in Cole-Cole plots.

Case Study 2 - PET Water Ratio

The study of water content in PET uses a narrower range of frequencies from 30kHz up to 200kHz. The buffer circuit was introduced to improve the output data straightness.

It is so performed a standard sweep for those frequencies and the resonance point is studied in changing frequencies.

Case Study 3 - Malaria Disease

In malaria case both the methods are used. The sweep is started in order to choose the best frequency to start a Single Frequency repeat acquisition. The results for Single Frequency varying the electrical-magnetic field angle are studied.

It is important to note that every acquisition was made outside and inside a magnetic field in eight orientations: 0°, 45°, 90°, 135°, 180°, 225°, 270°, 315°.

These orientations are relative to the electric field. Considering a current is generated between the two electrodes, the magnetic field starts parallel to this current (0°) and then it rotates 45 by 45 degrees till it completes 360 degrees rotation.

The results are dependent on the temperature, so this parameter was frequently measured to filter any artefact. The results obtained are shown hereafter in this dissertation.

Chapter 5

Results and Discussion

The results obtained, following the methods described above, will be presented in this chapter. The results are divided by the case study which it refers to. First, temperature sensor calibration tests are presented. Second, the results for Water Contamination will be presented followed by the results for PET/water ratio and Malaria.

5.1 Temperature Sensor

Due to the high influence of temperature in impedance results, a thermal sensor was tested in order to be added to the system in the future allowing the normalization of the impedance measurement.

In order to obtain temperature values through output voltage, an extrapolation was made using PT1000 data sheet [49]. This relation is represented in the graphic of Figure 5.1. Thus, the temperature can be calculated by $T = 0,0039 \times V_{out} + 1,0003$.

After that the room temperature was measured with a laboratory thermometer and compared with the PT1000 results. The linearity of the resistance with temperature was also studied. The results are presented in Figure 5.2 which confirms this linearity with enough accuracy. The relation between room temperature and the temperature obtained by PT1000 is given by $T_{PT1000} = 1,0513 \times T_{room} + 15,8302$. Linear regression was performed using an in-house program (available in the web page of the Physics Department of UC www.fis.uc.pt) for higher precision.

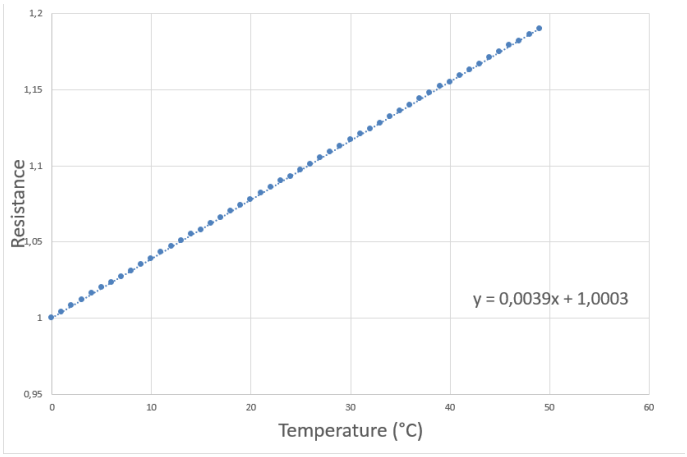

Figure 5.1: PT1000 temperature rate - linearity of resistance variation with temperature variation.

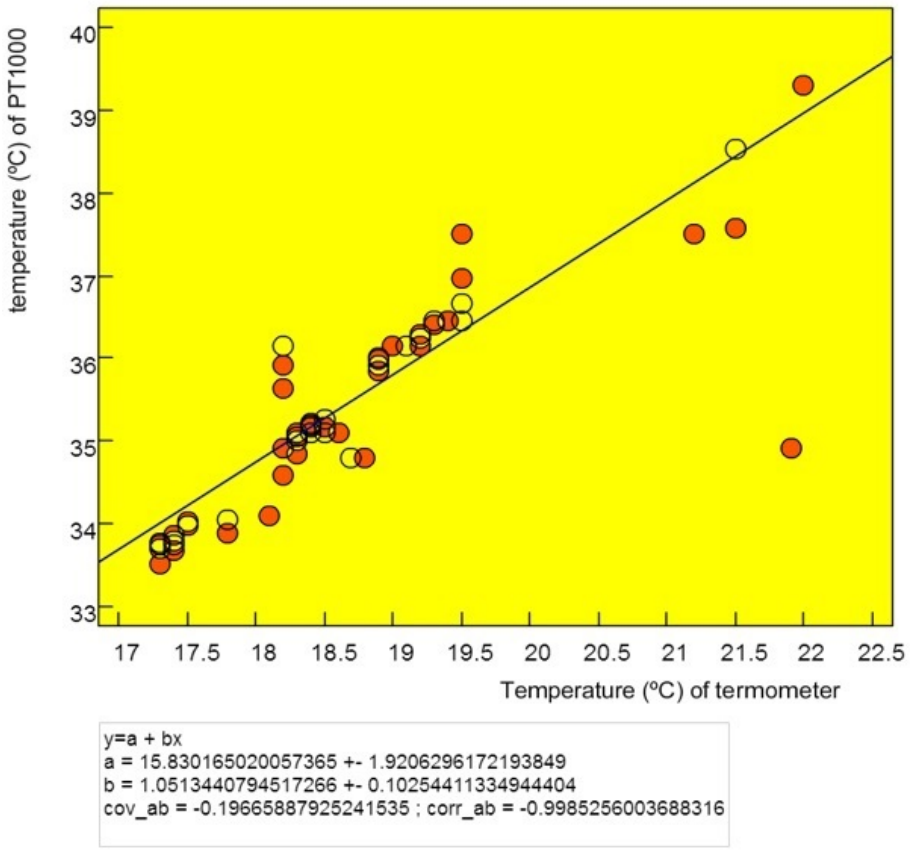

Figure 5.2: PT1000 linearity: Representation of PT1000 results according to the room temperature measured by a bench thermometer. The points are represented by red circles (colour changes to yellow when overlapping).

5.1.1 Discussion

With the tests described above it is possible to ensure PT1000 is a fundamental piece for data processing of the temperature.

The results shown, confirm the linearity of the PT1000 resistance, revealing however a difference of about 16 from room temperature. Once this difference is always present, it is therefore considered a systematic error, easy to overcome.

5.2 Case Study 1 - Water Contamination

In this section it is shown that, according to the EIS approach earlier studied, applying the standard sweep to distinguish their constituents, it is sufficient to know for each frequency the values of impedance and phase shift angle [1].

Water-tests were used initially for instrument calibration, being however found a potential application for the detection of contaminants in waste water or household water. Thus the tests proceeded and its results are presented hereafter.

The first results obtained to water, for the first electrode configuration used (A4 80 steel screws), are represented in Figure 5.3. In the first column, MI acquisitions are presented and in second column MV is shown. These results were obtained with impedance meter 1.

Figures 5.3(a) and 5.3(b) represent the impedance modulus for each mode. This modulus is higher as lower is the ionic concentration in water as presented in Table 4.1. Data is consistent for each MI and MV.

In Figures 5.3(c) and 5.3(d) the $\measuredangle Z$ is represented. It is possible to observe a higher phase variation for deionized water. For low and high frequencies, phase variation is more evident.

In Figures 5.3(e) and 5.3(f) is the Cole-Cole diagram representing the resistance and reactance relation of the fluid. It is possible to observe clearly one relaxation period for deionized water (more visible in MI than in MV). The Impedance meter 1 has some troubles in discern abrupt changes, easily introducing errors in the output voltage. Then, it is observed the *hook effect* for low frequencies, expressed in an unexpected reduction in resistance with increasing reactance followed by decrease of reactance as represented in

both modes.

The high susceptibility to errors of the device 1, manifested in the 3/4 repetitions of acquisitions, led to the need of producing a new impedance meter. After practical tests dictate the uselessness to the case, the use of a non-inverting mode, a new impedance meter based on the inverter mode have been printed on PCB, which resulted in much more accurate and reliable data, once with less noise and welding points.

The most accurate and conclusive tests performed with water using stainless steel wire as electrode are represented in Figure 5.4 for current mode. In this test four commercial waters were used: Fastio, Evian, distilled and deionized water. In the first instance it is possible to observe the graphs of impedance module in Figure 5.4(a). Such as in the last results, deionized water presents higher impedance modulus. All the water samples present a decrease in the impedance value up to $\sim 80Hz$, remaining constant thereafter up to frequency values $\sim 100kHz$. In Figure 5.4(b) the $\measuredangle Z$ is represented. Big differences in phase shift angle are observed for very low and very high frequencies. In Figure 5.4(c) is the Cole-Cole diagram representing the resistance and reactance relation of the fluid. It is possible to observe, as related in literature, the one relaxation semi-circle of deionized water [35, 37, 52].

Some outliers occur in MV acquisitions. Nevertheless MI and MV are coherent as shown in Figure 5.5. In this figure there are represented the impedance modulus, impedance phase shift angle, and Cole-Cole diagram, for deionized water in both MI and MV. It is possible to observe through the Cole-Cole diagram, the differences between the modes occur mainly in resistance in a discrepancy of nearly $2k\Omega$.

5.2.1 Discussion

Impedance values obtained are consistent with the ion variation presented in the waters under study. With $|Z|$ it is possible to discriminate with confidence different impedance levels for each of the water. This impedance variation is related to the ionic composition of water. The more ions are present in solution, the lower the impedance value due to the increased conductivity. Ionic mobility has also high influence in current conductivity [3, 53, 54].

Mobility parameter is one that justifies the variation of impedance modulus. Varying

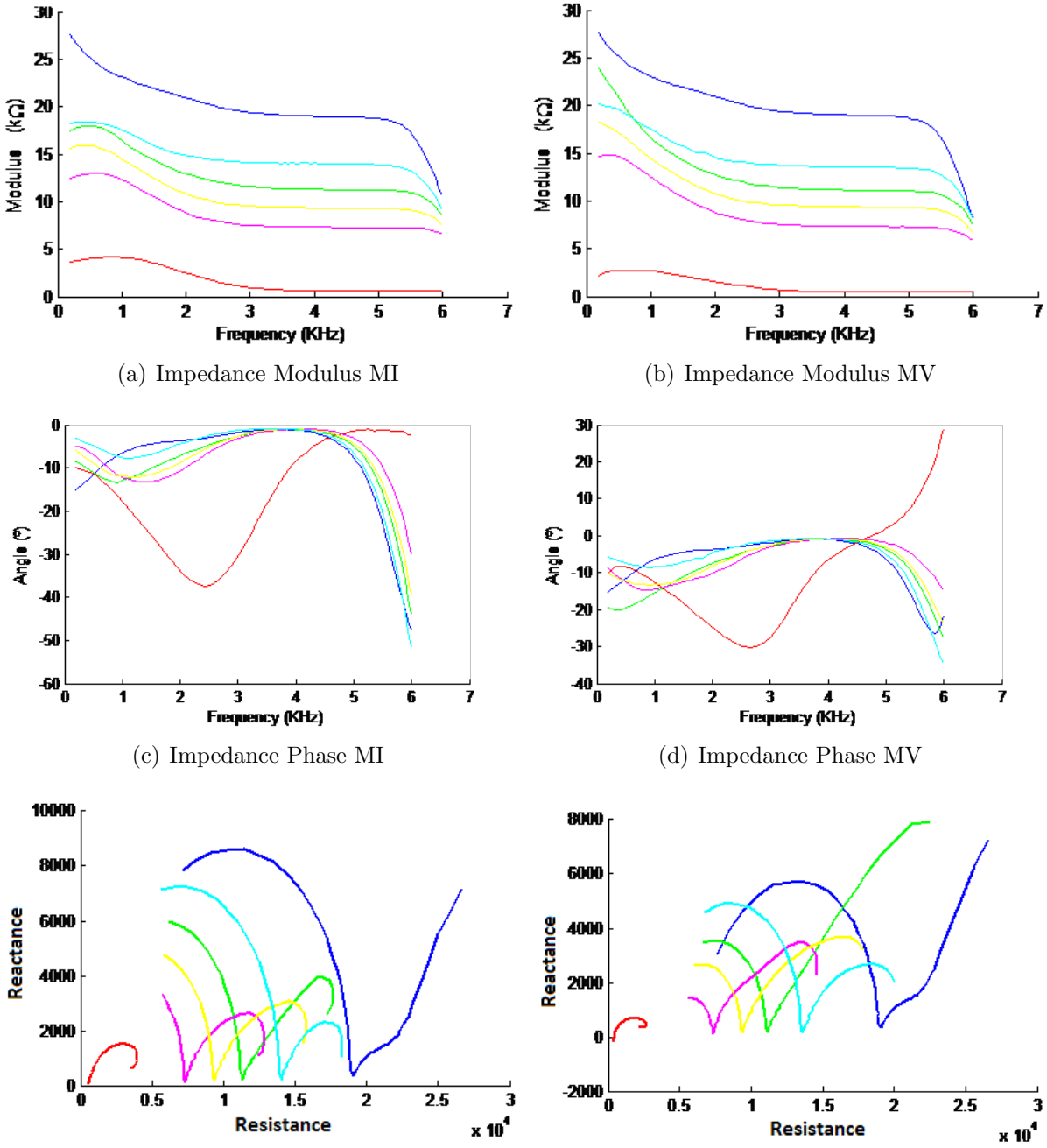

(a) Impedance Modulus MI

(b) Impedance Modulus MV

(c) Impedance Phase MI

(d) Impedance Phase MV

(e) Cole-Cole Diagram MI

(f) Cole-Cole Diagram MV

Figure 5.3: Graphical representation of different waters' impedance results for steel A4 80 electrodes: in dark blue – distilled water; in red – deionized water; in green Fastio; in magenta – Vimeiro Lisa; in yellow – Luso; in light blue – Vitalis. These water's ionic information is in the Table 4.1.

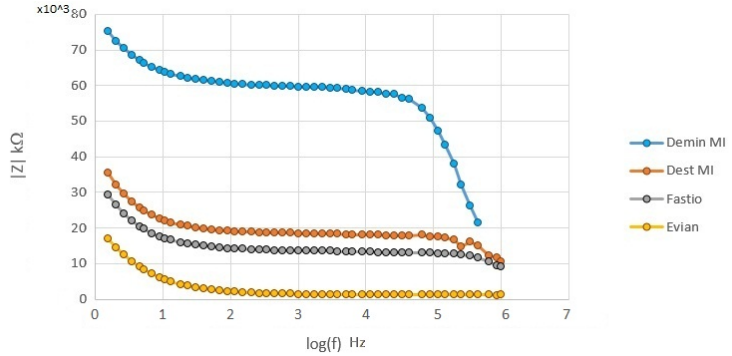

(a) Water Impedance Modulus MI

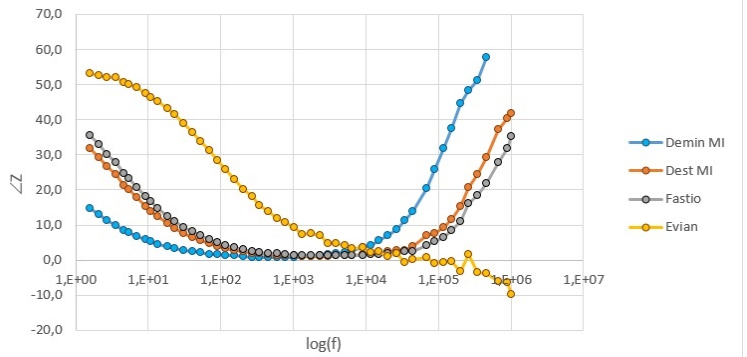

(b) Water Impedance Phase MI

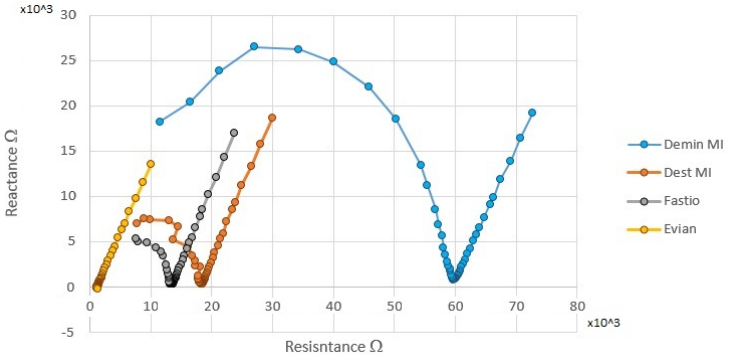

(c) Water Cole-Cole Diagram MI

Figure 5.4: Graphical representation of different waters' impedance results for current mode with low volume sample holder and wire cuvette 4: in 5.4(a) the $|Z|$; in 5.4(b) the $\measuredangle Z$; in 5.4(c) the Cole-Cole diagram. Deionized, distilled, Fastio and evian waters were tested.

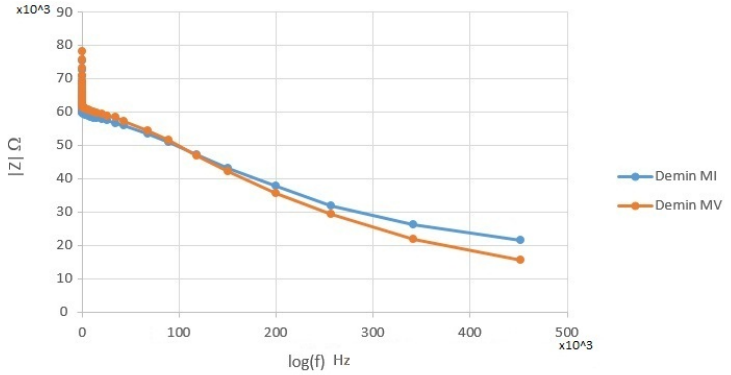

(a) Impedance Modulus MI—MV

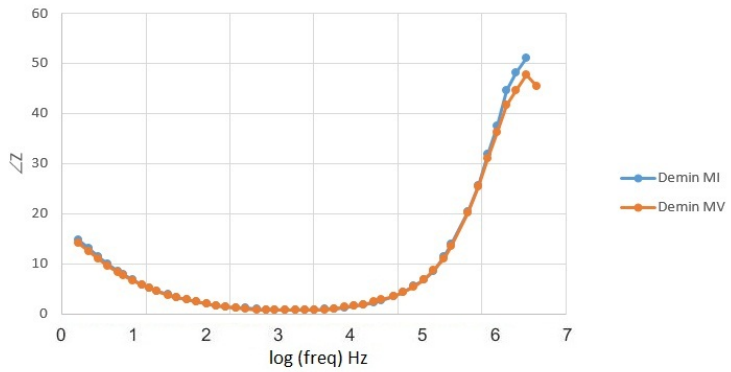

(b) Impedance Phase MI—MV

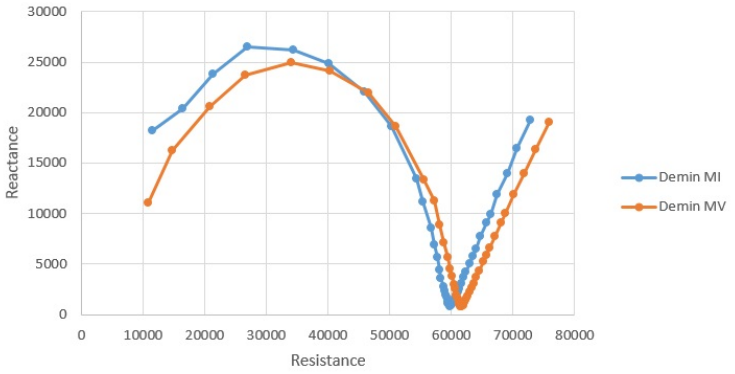

(c) Cole-Cole Diagram MI—MV

Figure 5.5: Comparison between MI and MV with representation of impedance modulus, phase shift angle and Cole-Cole diagram for demineralized water.

Table 5.1: Water ionic mobility results based on [54].

	$\mathbf{u}/(10^{-8}m^2s^{-1}V^{-1})$
H^+	36.23
Na^+	5.19
K^+	7.62
Zn^{2+}	5.47
OH^-	20.64
Cl^-	7.91
Br^-	8.09
SO_4^{2-}	8.29

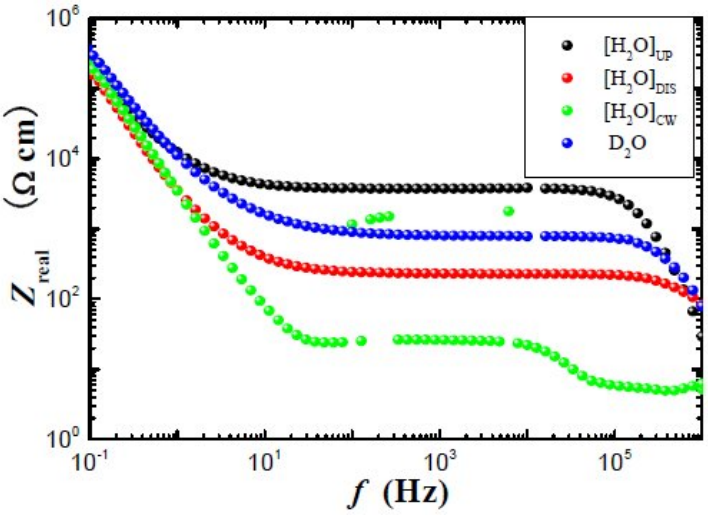

Figure 5.6: Water impedance results from [52].It represents impedance modulus for 3 waters from different sources (ultra pure, distilled and city water) and for deuterium oxide

the ionic concentration in the water, ohmic resistance increases or decreases in inverse proportionality. Consulting the Table 5.1 it is possible to observe this information.

They are also consistent with previous results from Abe [52] shown in Figure 5.6. The impedance modulus value is variable with the electrode shape and area [55]. This way it is important to observe that both the method of Abe [52] and ours result in the same impedance behaviour.

The last tests including waters were also consistent with the first ones and with the ones in the literature. Evian type of water has a behaviour close to a short circuit, getting close to a null impedance for higher frequencies.

For the Cole-Cole diagrams, it is possible to observe, as relater in literature, the one

relaxation semi-circle of deionized water [35, 37, 52].

The greatest amount of information about the fluid lies in Cole-Cole diagrams, whereby noticeable variation of the resistance to ionization - increased ionic concentration translates into greater variation of the resistance, each pair of ions introduces a discontinuity in the growth of reactance for a particular frequency.

Regarding Figures 5.3 and 5.4, it is possible to notice that MI has close results. Thus MV will be skipped in upcoming tests.

5.3 Case Study 2 - PET Moisture

In this section it is shown that, according to the EIS approach, applying the standard sweep with restrict frequencies (between 30kHz and 200 kHz) to determine the content of water in the PET samples, it is sufficient to know the values of output voltage and study its resonant frequency.

Once PET presents very low conductance which results in a very high impedance, it became necessary to increase the electrode area, which varies with inverse proportionality to the impedance module. Thus, first tests were performed with stainless steel rods, presenting very high impedance values, and a second set of tests are using stainless steel plates.

In the first instance it was considered important to assess the influence of the shape of pellets in the impedance module. The results are shown in Figure 5.7. In a second instance it was studied the variation of the resonance frequency with the ability to the passage of electric current. For this, the output signal V_{out} is rated to a narrower range of frequencies (between 30k and 200k). Seventy seven frequencies are evaluated as well, concluding a maximum voltage for the MI and a minimum for the MV. The MV has many artefacts, so that for this assessment was considered unnecessary, given the good results obtained in MI. The resonant frequency for PET is approximately 9 kHz higher than for air as shown in the graphic of Figure 5.8. This difference has a significant importance since there is a possibility to study resonance in order to distinguish material properties.uy

In order to study impedance variations with the water ratio in PET. It was wet up to the saturation humidity (it did not absorb/adsorb more and released excess). Drying was

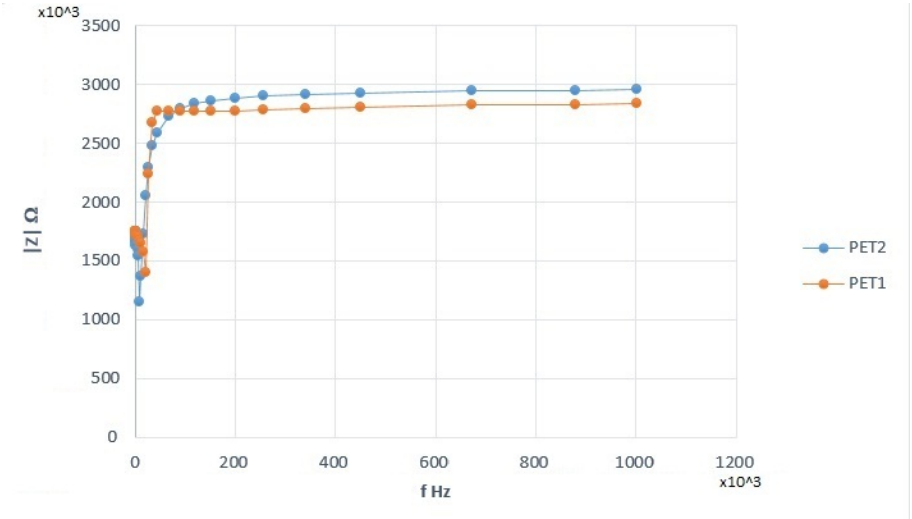

Figure 5.7: Comparison between PET1 and PET2 impedance modulus considering the same conditions of acquisition

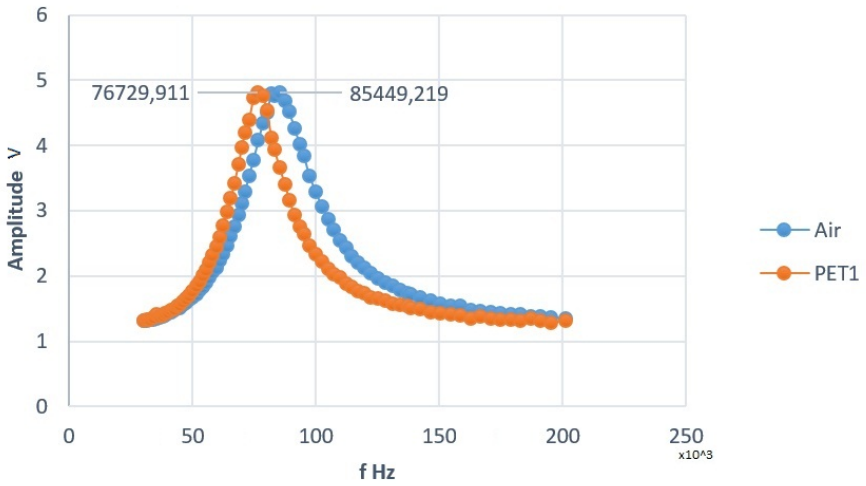

Figure 5.8: Comparison between the ressonance frequency for PET and the one obtained without the PET charge between the electrodes - background.

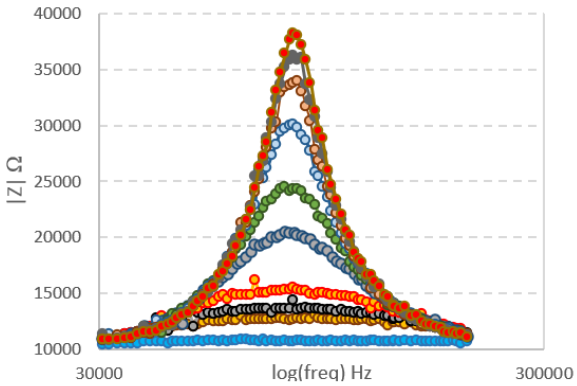

(a) Impedance Modulus MI

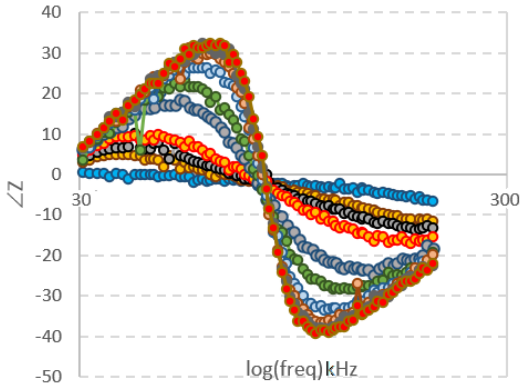

(b) Impedance Phase MI

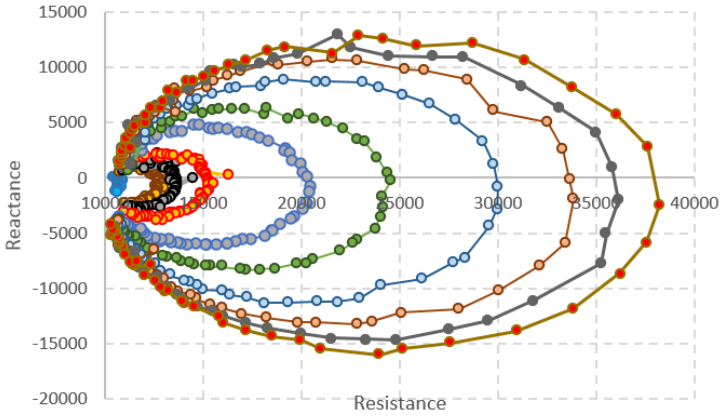

(c) Cole-Cole Diagram MI

Figure 5.9: Evolution of PET impedance as it dries from water-saturated (light blue) to almost dry (red). The colours presented in the middle were randomly chosen and they are time dependent and constant.

done at room temperature and the amount of water monitored by a scale. The impedance measurements occur in parallel with the water weight loss measurement which allows us to relate these values.

The measurements obtained are represented in Figure 5.9. Figure 5.9(a) presents impedance module, Figure 5.9(b) presents the impedance phase shift angle and Figure 5.9(c) the Cole-Cole diagram. The different colours shows time evolution of drying process from light blue to red, in the order presented. It is possible to observe an increasing of Impedance modulus peak with the dry process. Impedance maximum is coincident with the phase shift annulment, with a value around $85kHz$.

5.3.1 Discussion

In the first instance it was considered important to assess the influence of the shape of pellets in the impedance module. The results suggest that the shape of the pellets does not significantly influence the ability of PET to halting the driving current.

Once considering the PET as a buffer resonant circuit, we tried to find the frequency for which the impedance of the PET is cancelled. The results obtained in Figure 5.8 shows that there is a frequency maximum for resonance around $85kHz$. Nevertheless, impedance study will provide more information concerning the physical behaviour of the material, so the study of the material water content distinction proceeds by this part. It is possible to study the conversion of resistive behaviour to capacitive behaviour of PET. The important frequency for that is resonance frequency around $85kHz$.

Last tests included PET wetting until water saturation and to observe its behaviour throughout its drying. Drying was done at room temperature and the amount of water monitored by a scale. PET resistance evolves from short-circuit in the water saturation (light-blue curve) to very high values in the dry PET (red curve) as shown in Figure 5.9.

Water absorption in 24 hours is 0.1% [56]. The drying process starts with adsorbed water evaporation which is quicker than the absorbed water evaporation. Thus the water weight loss is more rapid in first hours. It is possible to observe a constant relation between resistance and reactance due to dry evolution. It is possible to find a relationship between the resistance and the reactance, and thus determine the amount of water present in the sample.

5.4 Case Study 3 - Malaria Disease

In this section it is shown that, according to the EIS approach, applying both the standard sweep and the single frequency methods to detect the presence of hemozoin in blood, are crucial to know the impedance of the fluid and to study the influence of the magnetic field in the impedance, differentiating the presence of ferromagnetic material.

Rabbit blood was used to test the influence of fluid viscosity in impedance modulus before the study with human blood. These tests were made in order to understand the meaningful parameters to further speed up the processing of data to human samples.

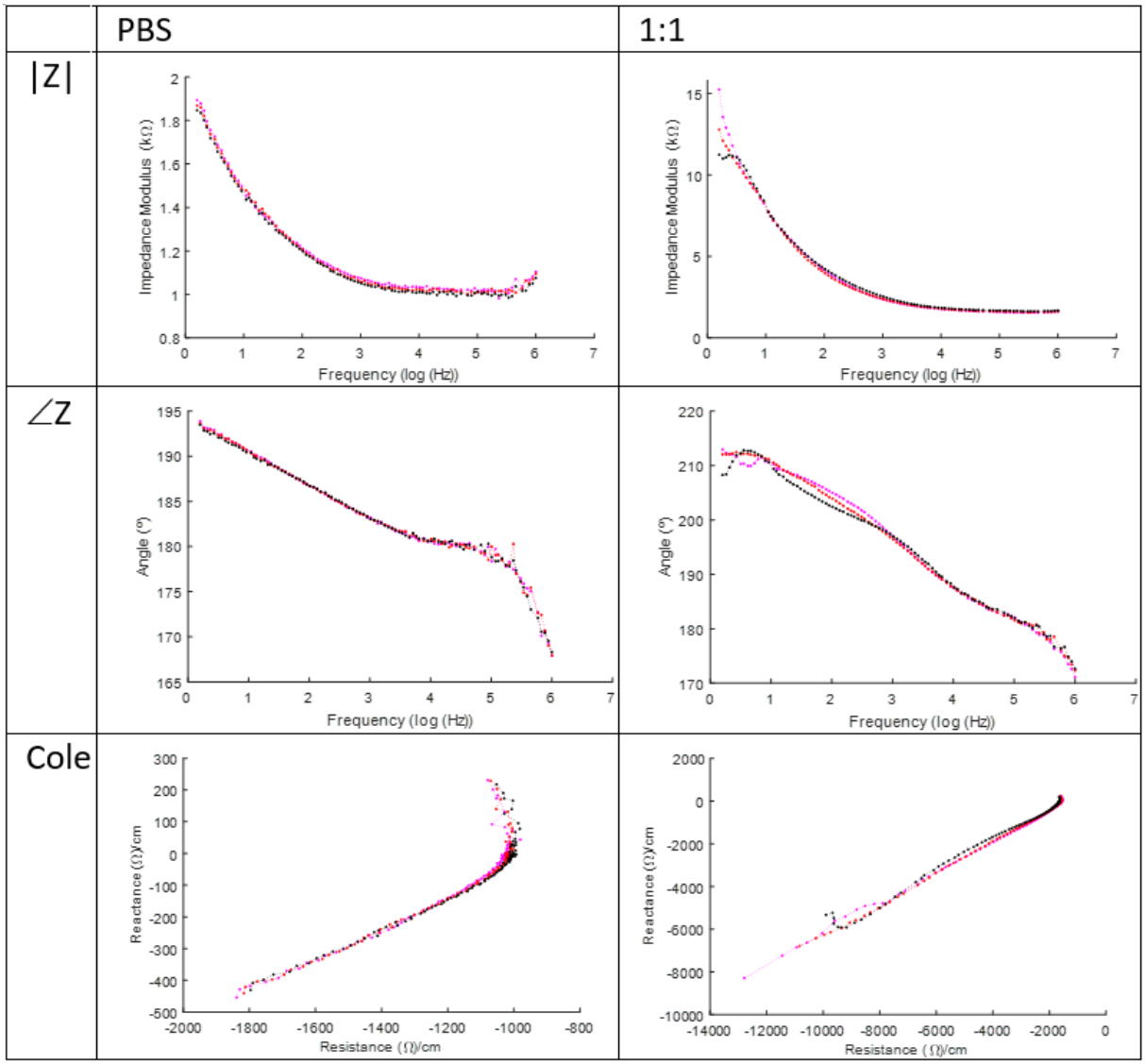

Figure 5.10: Results for for PBS and PBS:Blood (1:1) dilutions. Magenta dots refer to acquisition without magnetic field, red dots to 0 degree field and black dots to 90 degree field.

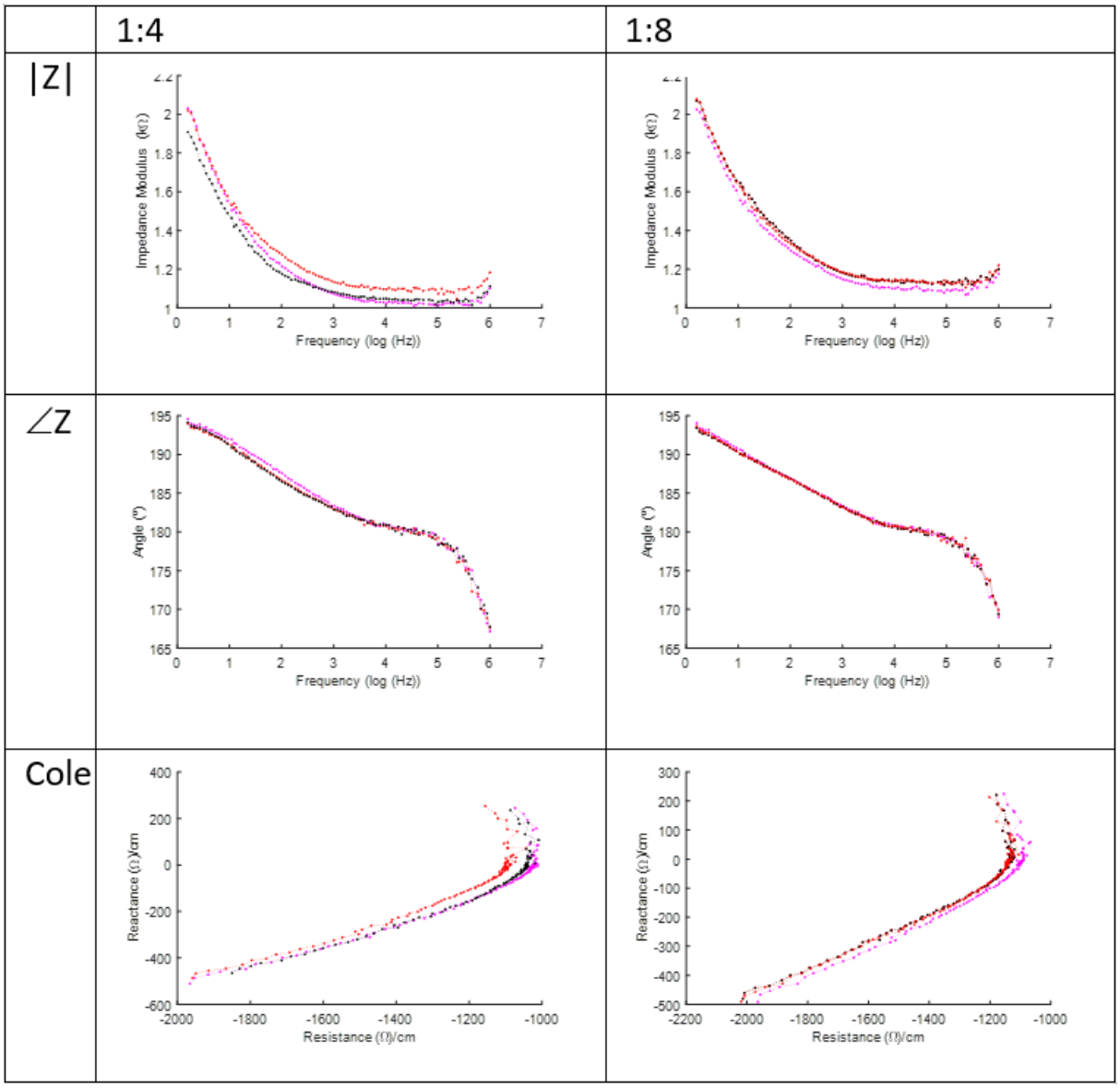

Figure 5.11: Results for for PBS:Blood (1:4) and PBS:Blood (1:8) dilutions. Magenta dots refer to acquisition without magnetic field, red dots to 0 degree field and black dots to 90 degree field.

That said, the initial tests aimed to understanding what the best ratio of PBS-blood to make possible to dilute the blood, and with it, spend a smaller blood amount. The results are shown in Figures 5.10 and 5.11. The concentrations used are also referred in Table 4.2.

The graphic is representing three states: magenta dots refers to acquisition without magnetic field, red dots to 0 degree field and black dots to 90 degree field. It is presented in the first raw the impedance modulus results, in the second raw the impedance phase shift angle and as last the Cole-Cole diagram.

When more diluted than 1:1, impedance spectrum is closer to PBS (pure) spectrum than to blood (pure) spectrum, which means that PBS characteristics override the resistive properties of blood. Once selected the best concentration of the blood-PBS, in this case 1:1,the maximum acceptable, it began the introduction of synthetic hemozoin in blood (1:1 PBS). It was also made a study of the minimum proportion required for HZS to be detected by the method, and also what changes happen in their behaviour in the presence of a magnetic field of about 1/3 T. The results are presented in Figures 5.12 and 5.13.

The graphic is representing three states: magenta dots refers to acquisition without magnetic field, red dots to 0 degree field and black dots to 90 degree field. It is presented in the first raw the impedance modulus results, in the second raw the impedance phase shift angle and as last the Cole-Cole diagram.

After a quick analysis of these results it was decided to use the dilution of $1 : 1$ of the blood with PBS. After that, human blood samples were studied. The last tests were performed with INML support: 9 samples of human blood were manipulated in the custody of INML CF central delegation, and this blood was unidentified, hemolysed and treated with Potassium Fluoride and Na_2 EDTA. At first a comparison between the 9 blood impedance sweep for all the frequency range 1Hz-1MHz was made. The results are presented in Figure 5.14. It is possible to observe that each blood sample has its identity, getting different impedance values for low frequencies.

From this results, and supporting the previous ones with the rabbit blood, it was considered important to test single frequencies around $100Hz$. The main test consists in laying the fluid in the Halbach and to acquire some points per minute to each angle. When the acquisition finishes, Halbach is rotated to the initial position (zero degree) and

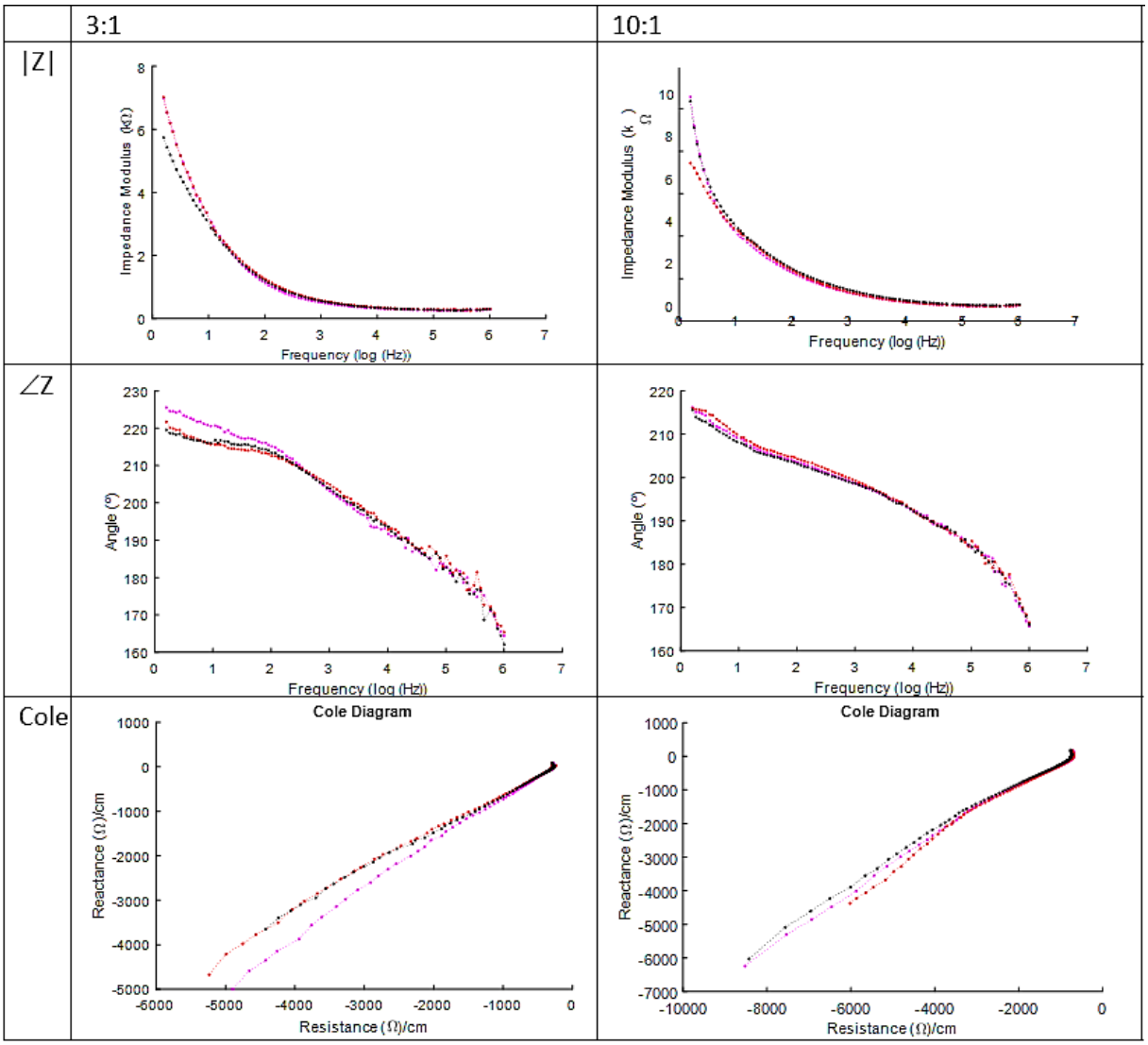

Figure 5.12: Results for Blood:HzS dilutions (3:1) and (10:1).Blood is presented in a dilution Blood:PBS (1:1). Magenta dots refer to acquisition without magnetic field, red dots to 0 degree field and black dots to 90 degree field.

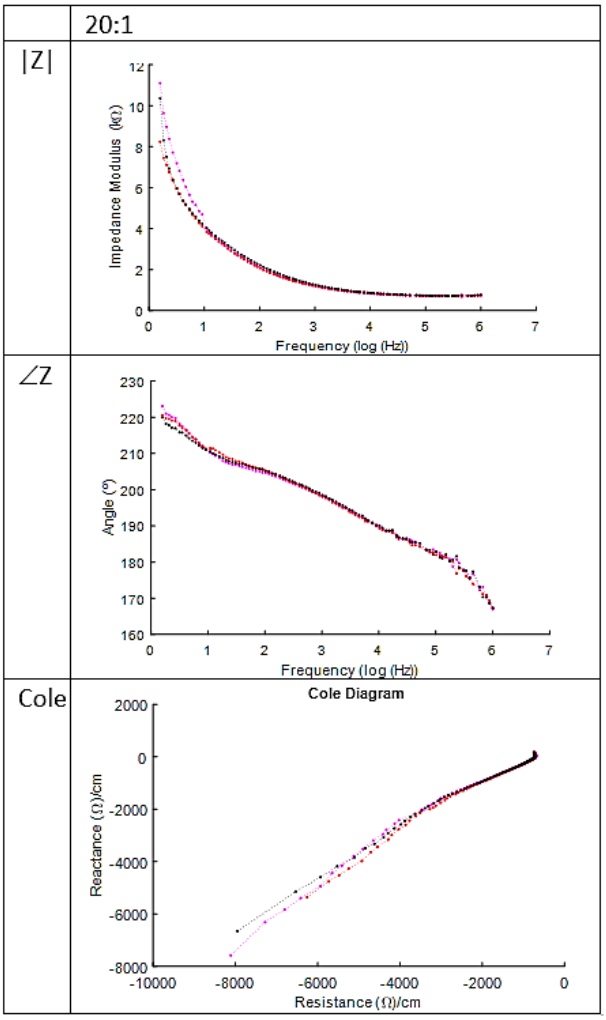

Figure 5.13: Results for Blood:HzS dilutions (20:1).Blood is presented in a dilution Blood:PBS (1:1). Magenta dots refer to acquisition without magnetic field, red dots to 0 degree field and black dots to 90 degree field.

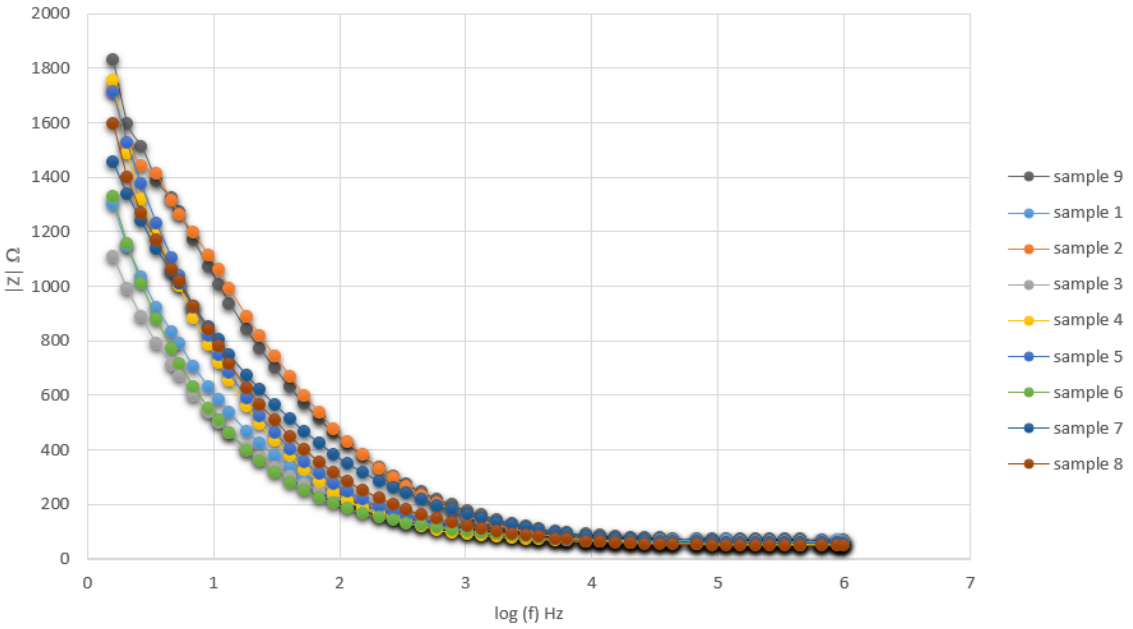

Figure 5.14: Graphical representation of different bloods' impedance results for current mode with low volume sample holder and wire cuvette 4 using standard sweep method for frequency range 1Hz-1MHz. Blood is diluted with Blood:PBS (1:1)

it is rotated to the next angle after 5 minutes. Thus, the results for this experiment are presented in Figures 5.15, 5.16 and 5.17. It is possible to observe the impedance modulus and the phase shift angle for each of the 9 samples used diluted 1 : 1with PBS. It is also remarkable the dependence of these parameters with the Halbach's angle. Healthy blood does not present a significant change while rotating Halbach cylinder.

Some tests were performed in order to understand hemozoin behaviour in relation with the magnetic field's rotation. The main test consists in lay the fluid in the Halbach and acquire some points per minute to each angle. When the acquisition finish, Halbach is rotated to initial position (0 degree) and rotated to next angle after 5 minutes.

The results for the HzS with the concentration of $1mg/ml$ are represented in Figure 5.18. It is possible to observe, in general, the time to reach equilibrium gets high as the angle increases.

5.4.1 Discussion

Observing Figure 5.10 it is possible to understand, by the three colours almost always overlying each other, that the magnetic field has no influence in rabbit blood samples

without HzS. From the first study it was observed that for dilutions superiors to 1:1 with PBS, the blood starts having less significance. Thus, it was considered the maximum dilution, used for the following tests. The presence of HzS changes the impedance values with the rotation of the magnetic field. This differences are more visible for low frequencies as observed for maximum concentration 3:1 (blood:HzS) in Figure 5.12.

Then, human blood samples ceded by INML CF were studied. These samples were initially placed under a **standard sweep** test to understand how to choose the best frequency to **single frequency** tests with rotation of the magnetic field. From the obtained results withdraws the information that every blood is a different case, with altogether contrasting properties, so that, especially for low frequencies, has very distinct values.

Considering the low frequencies between 10 and 100 Hz and taking into account the amplitude of the output signal or saturation thereof, frequency of 100 Hz was selected for the following tests. This often ensures a certain distinction between bloods, as observed in Figure 5.14.

Proceeding to single frequency, Figures 5.15, 5.16 and 5.17 results are quite consistent with expectations: the impedance module is substantially constant over time and the phase shift angle suffers small non-significant variations.

When studying pure HzS with concentration $1mg/ml$, presented in Figure 5.18, it reveals a transitional regime in first minutes. This transitional regime can be associated to the rotation of the ferromagnetic rods. On the other hand, healthy blood does not present a significant change while rotating Halbach cylinder. This results were expected since hemoglobin does not have ferromagnetic properties as the parasitized cells - hemozoin.

It is important to note that the concentration of HzS under study ($1mg/ml$) is much higher than the expected maximum concentration in blood. It was made a broadening of the signal in order to understand their behaviour in the presence of a variable magnetic field.

Through the literature, it is possible to expect an alignment of the rods with the direction of the magnetic field, so that this change is related to the relaxation of the impedance of the fluid stream. [16, 23, 33]. It is expected that the stream follows the path of highest magnetic permeability, so that it arrives more intensely when the electric field and the magnetic field are aligned. What is observed are certain adjustments in the

rotation. The explanation proposed for this movement is a torque variation during the rotation of the rods to align with the magnetic field.

Since the magnetic field starts the rotation from the 0 degree position, the impedance variation is interpreted as an internal movement of fluid due to the rods alignment. This movement manifested itself quite complex. Clearly it only shows the presence of ferromagnetic materials.

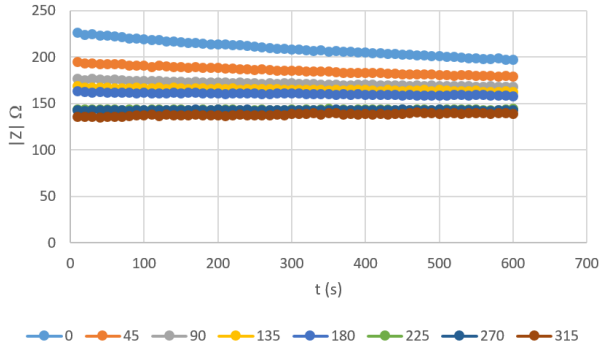

(a) Sample 1 Impedance Modulus

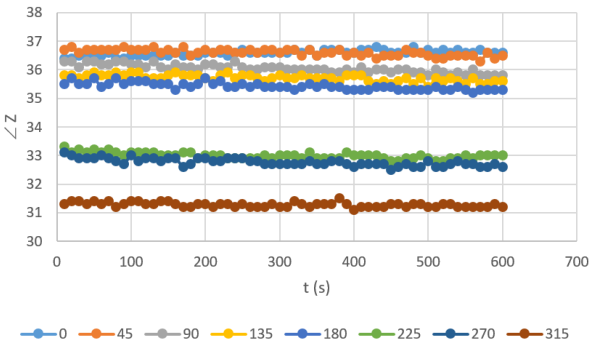

(b) Sample 1 Impedance Phase

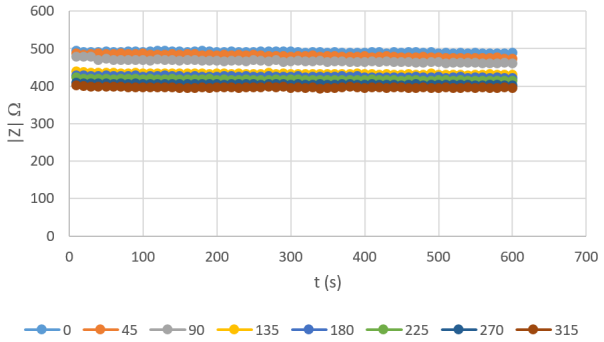

(c) Sample 2 Impedance Modulus

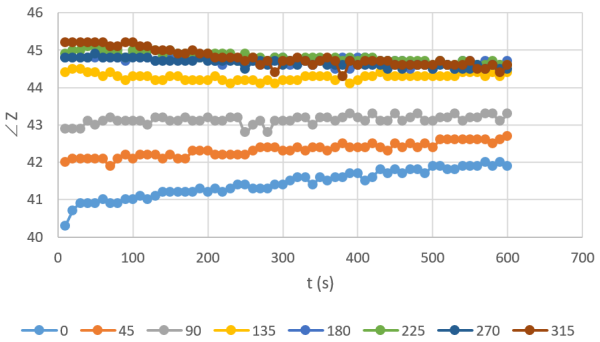

(d) Sample 2 Impedance Phase

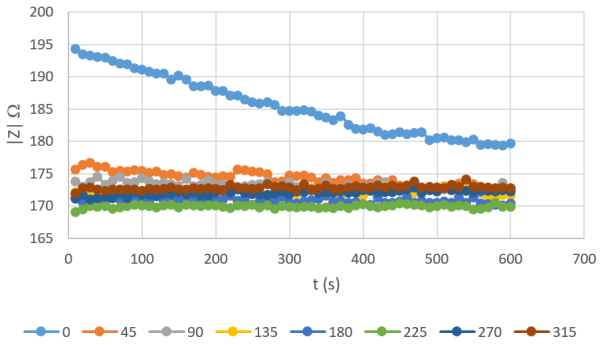

(e) Sample 3 Impedance Modulus

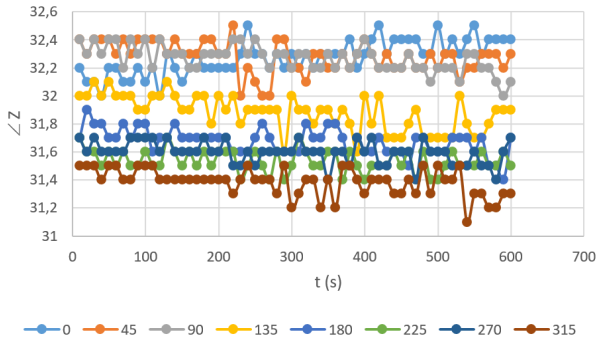

(f) Sample 3 Impedance Phase

Figure 5.15: Graphical representation of samples 1, 2 and 3 impedance results for current mode with low volume sample holder and wire cuvette 4: the $|Z|$ and the $\measuredangle Z$ for the $f = 100Hz$.

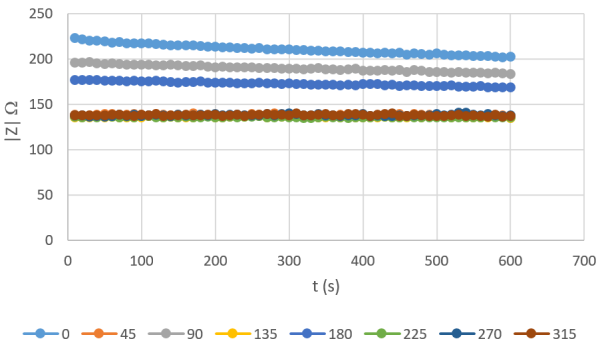

(a) Sample 4 Impedance Modulus

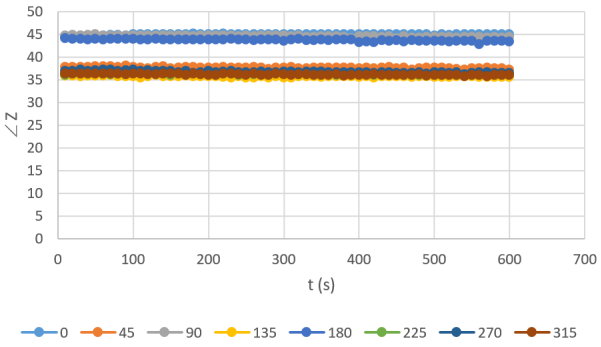

(b) Sample 4 Impedance Phase

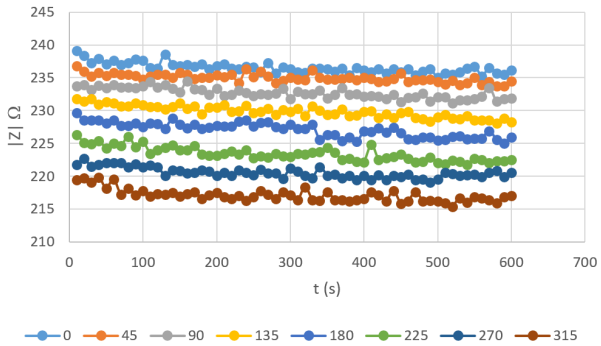

(c) Sample 5 Impedance Modulus

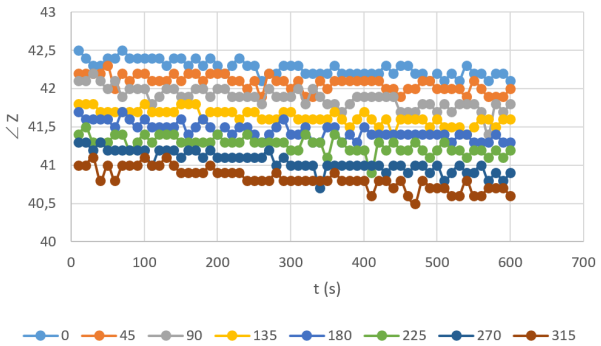

(d) Sample 5 Impedance Phase

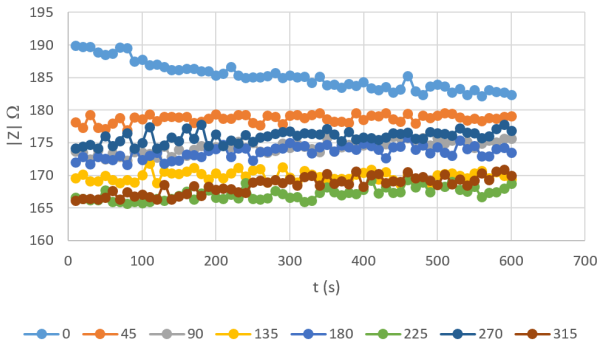

(e) Sample 6 Impedance Modulus

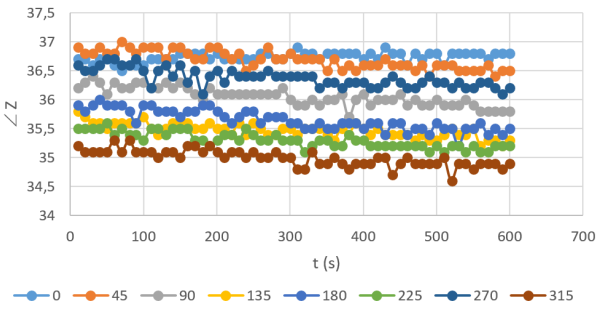

(f) Sample 6 Impedance Phase

Figure 5.16: Graphical representation of samples 4, 5 and 6 impedance results for current mode with low volume sample holder and wire cuvette 4: the $|Z|$ and the $\angle Z$ for the $f = 100Hz$.

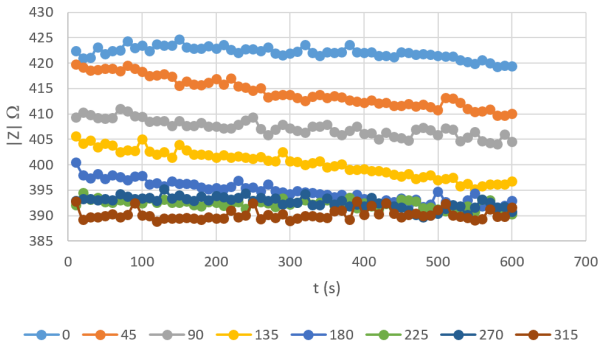

(a) Sample 7 Impedance Modulus

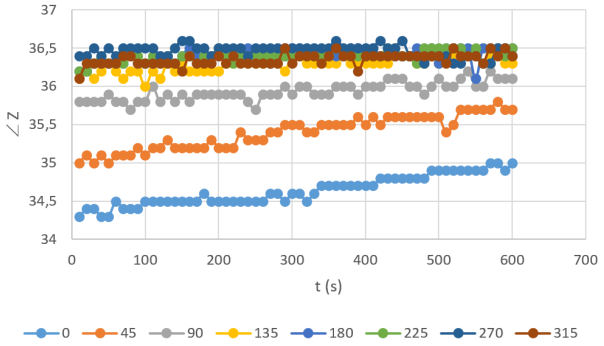

(b) Sample 7 Impedance Phase

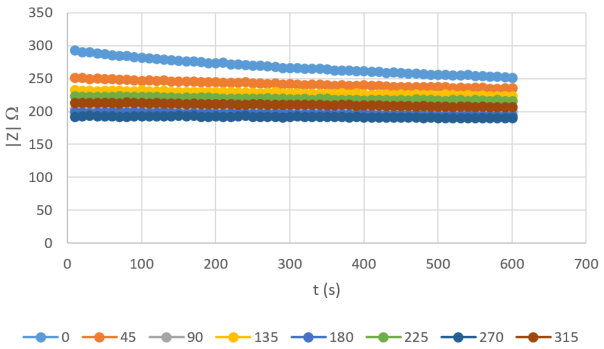

(c) Sample 8 Impedance Modulus

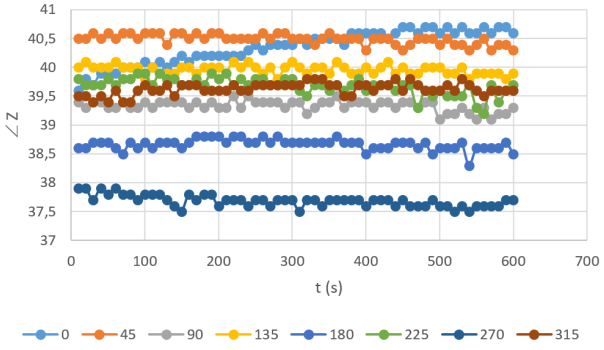

(d) Sample 8 Impedance Phase

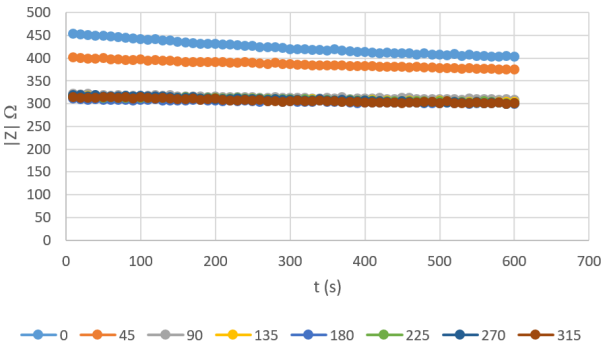

(e) Sample 9 Impedance Modulus

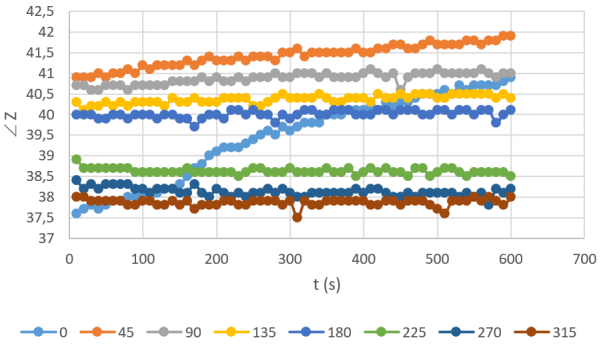

(f) Sample 9 Impedance Phase

Figure 5.17: Graphical representation of samples 7, 8 and 9 impedance results for current mode with low volume sample holder and wire cuvette 4: the $|Z|$ and the $\measuredangle Z$ for the $f = 100Hz$.

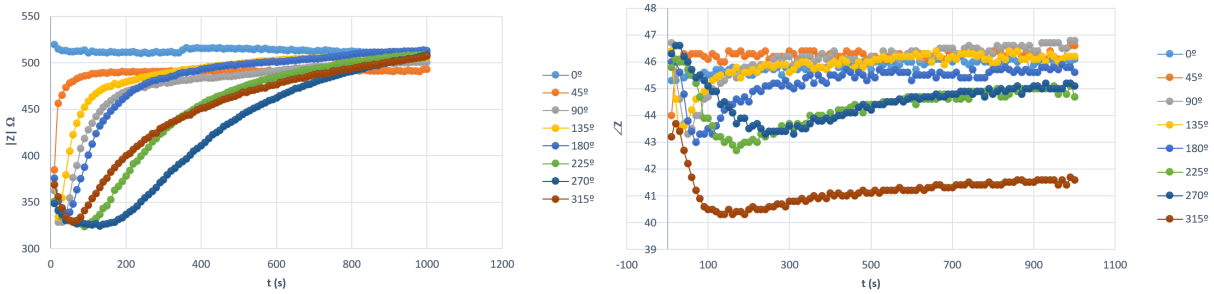

(a) Impedance Modulus

(b) Impedance Phase

Figure 5.18: HzS magnetic behaviour with the $1/3T$ Halbach: the impedance modulus and impedance phase shift angle for HzS $1mg/ml$.

Chapter 6

Conclusions

The main advantages of the device developed and the EIS method are the simplicity for the user, its inexpensiveness and its accuracy. It is able to give relatively quick and accurate results in the cases studied. The device is robust and it deserves a more thorough investigation. Thus the main conclusions for water contamination, PET moisture and malaria disease are presented in this chapter. The key aspects in order to continue the work carried out so far are finally referred.

The results are affected by the environmental temperature although it is possible to compare, for the same temperature, the resistance and reactance of the fluids and materials.

The study demonstrated the versatility of the apparatus and its possibility to adapt to water environment. By changing circuit internal parameters it is possible to distinguish with relatively good precision the commercial types of water. The conductance differences exist due to water ionic composition.

This method also showed accurate results for PET moisture: it is able to detect water presence in PET pellets since water alters material conductance.

EIS revealed to be a suitable method for detecting hemozoin pigments in small samples of hemolyzed whole blood (without separation of components).

6.1 Future Work

The tests performed during the master thesis were important in order to guide the future work to achieve the goals established initially. All the tests developed and presented above indicate that the final purpose can be achieved, considering the time necessary for the device conception and optimization. It is expected that malaria detection technique becomes a non-invasive method with this device which performs the uncovering of the parasite through patient's skin without the need of blood collections.

Some characteristics are important to determinate the relevance of the device to these applications:

- **Better autonomy**: The impedance meter device should be fully portable and use a battery as a power supply;
- **Short analysis time**: The analysis time in the final prototype should be shorter than 5 minutes;
- **Low cost of operation**: The total process, including the device production and maintenance and the disposable components, must be the least expensive;
- **Low electric consumption** Batteries lifetime must handle a large number of acquisitions without shut down the system;
- **Possibility of creation of a mobile interface**: The portability of the device is crucial to its applications. Thus the first tests are using Matlab although later an independent format can be used;
- **Versatile design**: In order to apply this device to several cases, its design configuration and software must be modifiable keeping its accuracy;
- **High robustness** The device must be in a box and withstand a hostile environment while maintaining their constant replies.

Thus some topics for future work are here proposed for hardware, software and future tests.

6.1.1 Hardware improvement

- The thermometer must be inserted in the system as a calibration instrument (the impedance must be normalized according to temperature);
- The linear magnetic field must be improved in order to obtain a high magnetic intensity in cylinder's centre. An inductive system can be a possible future bet;
- The final circuit power supply must be optimized in order to use a battery getting fully portable properties. It must be studied carefully in order to get high time autonomy;
- A commercial device must be produced in order to replace the usage of the personal computer as the interface and go on to have a device with all the embedded processing: development of an interface and independent controller;
- Input mode of the fluid in the container should be more practical and adapted to the user's needs - larger aperture above and adaptable to pipettes;
- cuvette fitting mode must be optimized to decrease user efforts.

6.1.2 Software

- Cole-Cole diagram should suffer mathematical processing in order to study curve magnitudes and distinguish components through mathematical approximation. The relation resistance-reactance is considered crucial;
- Software must present only final aim to the user as the contaminated/non-contaminated in water, moisture level in PET and infection/non-infection in malaria. It must be user-friendly.

6.1.3 Future Tests

- Different contaminants must be introduced in water tests in order to outwit their influence in fluid conductance;

- PET moisture is fully related with the resistance of the material to current. Next steps can study and quantify this relation varying surrounding parameters (air humidity, temperature and pressure) in a controlled environment;
- Tests with infected blood must be performed to study EIS prototype's sensitivity and specificity.

Bibliography

[1] George Tchobanoglous, Fl. Burton, and H. David Stensel. Wastewater engineering: An Overview. *Wastewater Engineering Treatment and Reuse*, pages 1–24, 1991.

[2] Lara Cerdeira. *Acompanhamento do Arranque /Exploração de uma ETAR*. PhD thesis, Universidade do Porto, 2008.

[3] Song Hi Lee and Jayendran C. Rasaiah. Molecular Dynamics Simulation of Ion Mobility. 2. Alkali Metal and Halide Ions Using the SPC/E Model for Water at 25 ℃. *Journal of Physical Chemistry*, 100(4):1420–1425, 1996.

[4] C.A. Velis. Global recycling markets - plastic waste: A story for one player China. *International Solid Waste Association - Globalisation and Waste Management Task Force*, pages 1–66, 2014. Accessed July 19, 2016.

[5] Chetna Sharon and Madhuri Sharon. Studies on Biodegradation of Polyethylene terephthalate: A synthetic polymer. *Journal of Microbiology and Biotechnology Research*, 2(2):248–257, 2012.

[6] CBL. Annual Report. 2015. Accessed July 20, 2016.

[7] Dauvergne and Peter. The Problem of Consumption. *Global Environmental Politics*, (May):28–29, 2010.

[8] National Center for Biotechnology Information. PET. https://pubchem.ncbi.nlm.nih.gov/compound/444075 . Accessed July 24, 2016.

[9] David Lazarevic, Emmanuelle Aoustin, Nicolas Buclet, and Nils Brandt. Plastic waste management in the context of a European recycling society: Comparing results and uncertainties in a life cycle perspective. *Resources, Conservation and Recycling*, 55(2):246–259, 2010.

[10] S. M. Al-Salem, P. Lettieri, and J. Baeyens. Recycling and recovery routes of plastic solid waste (PSW): A review. *Waste Management*, 29(10):2625–2643, 2009. Accessed August 30, 2016.

[11] Nanying Jia, Howard a. Fraenkel, and Val a. Kagan. Effects of Moisture Conditioning Methods on Mechanical Properties of Injection Molded Nylon 6. *Journal of Reinforced Plastics and Composites*, 23(7):729–737, 2004.

[12] American Plastics Council. Best Practices in PET Recycling. Technical report, 1997.

[13] Simar. The Drying of Engineering Plastics, consuled on 25-5-2015. Technical report.

[14] WHO. Who Report 2015. Technical report, 2015.

[15] Ana Margarida Ferreira Góis. *Production and Characterization of Different Types of Malaria Pigment (Hemozoin) and Their Potential Use for Screening for Hemozoin Inhibiting Drugs*. PhD thesis, 2012.

[16] a Butykai, a Orbán, V Kocsis, D Szaller, S Bordács, E Tátrai-Szekeres, L F Kiss, a Bóta, B G Vértessy, T Zelles, and I Kézsmárki. Malaria pigment crystals as magnetic micro-rotors: key for high-sensitivity diagnosis. *Scientific reports*, 3:1431, jan 2013.

[17] Maria Rebelo, Howard M. Shapiro, Teresa Amaral, José Melo-Cristino, and Thomas Hanscheid. Haemozoin detection in infected erythrocytes for Plasmodium falciparum malaria diagnosis-Prospects and limitations. *Acta Tropica*, 123(1):58–61, jul 2012.

[18] Patrick Duffy and Michal Fried. Malaria: New diagnosys for an old problem. *The American Society of Tropical Medicine and Hygiene*, 73(3):482–483, 2005.

[19] Noppadon Tangpukdee, Chatnapa Duangdee, Polrat Wilairatana, and Srivicha Krudsood. Malaria diagnosis: a brief review. *The Korean journal of parasitology*, 47(2):93–102, jun 2009.

[20] Bruce Alberts, Alexander Johnson, Julian Lewis, Keith Roberts, and Peter Walter. *Molecular Biology of the Cell*, volume 5. Fifth edition, 2008.

[21] National Institutes of Health (NIH). Life Cycle of the Malaria Parasite. http://www.niaid.nih.gov/topics/malaria/pages/lifecycle.aspx, 2009. Accessed August 30, 2016.

[22] Clotilde Ribaut, Karine Reybier, Olivier Reynes, Jérôme Launay, Alexis Valentin, Paul Louis Fabre, and Françoise Nepveu. Electrochemical impedance spectroscopy to study physiological changes affecting the red blood cell after invasion by malaria parasites. *Biosensors & bioelectronics*, 24(8):2721–5, apr 2009.

[23] Woosung Kim, Sahin Kaya Ozdemir, Jiangang Zhu, Monifi Faraz, Cevayir Coban, and Lan Yang. Detection and size measurement of individual hemozoin nanocrystals in aquatic environment using a whispering gallery mode resonator. *Optics express*, 20(28):29426–46, 2012.

[24] Monika Chugh, Vidhya Sundararaman, Saravanan Kumar, Vanga S Reddy, and Waseem A Siddiqui. Protein complex directs hemoglobin-to-hemozoin formation in Plasmodium falciparum. *Proceedings of the National Academy of Sciences*, 110(14):1–6, 2013.

[25] Elfrida M. Carstea, John Bridgeman, Andy Baker, and Darren M. Reynolds. Fluorescence spectroscopy for wastewater monitoring: A review. *Water Research*, 95:205–219, 2016. Accessed August 30, 2016.

[26] Marcela Seifrtova, Lucie Novakova, Celeste Lino, Angelina Pena, and Petr Solich. An overview of analytical methodologies for the determination of antibiotics in environmental waters. *Analytica Chimica Acta*, 649(2):158–179, 2009.

[27] INC. MEECO. Tracer 2 Modulator Moisture Analyzer.

[28] Hamid Farahani, Rahman Wagiran, and Mohd Nizar Hamidon. *Humidity sensors principle, mechanism, and fabrication technologies: A comprehensive review*, volume 14. 2014.

[29] P.M. Faia, C.S. Furtado, and a.J. Ferreira. AC impedance spectroscopy: a new equivalent circuit for titania thick film humidity sensors. *Sensors and Actuators B: Chemical*, 107(1):353–359, 2005.

[30] Pedro M. Faia, Juliano Libardi, and Cristina S. Louro. Effect of V2O5 doping on p- to n-conduction type transition of TiO2:WO3 composite humidity sensors. *Sensors and Actuators, B: Chemical*, 222:952–964, 2016.

[31] Anantha P. E Du, Sungjae Ha, Monica Diez-Silva, Ming Dao, Subra Suresh and Chandrakasan. Electric Impedance Microflow Cytometry for Characterization of Cell Disease States. *Lab Chip.*, 13(19):3903–3909, 2014.

[32] Dave M Newman, J Matelon, M Lesley Wears, and Luke B Savage. The In Vivo Diagnosis of Malaria : Feasibility Study Into a Magneto-Optic Fingertip Probe. *IEEE Journal of selected topics in quantum electronics*, 16(3):573–580, 2010.

[33] Gregory Stephen, Advisors Robert Deissler, and Robert Brown. *Rapid Malaria Detection using the Magneto-Optical Properties of the Malaria Pigment*. PhD thesis, 2014.

[34] Simão Nunes Paula. *Exploring impedance spectroscopy as a mean of malaria diagnostic Biomedical Technologies*. PhD thesis, 2014.

[35] J R Macdonald. Impedance spectroscopy. In *Annals of Biomedical Engineering*, volume 20, pages 289–305. 1992.

[36] Sen-ben Liao, Peter Dourmashkin, and John Belcher. Chapter 12 Alternating-Current Circuits. pages 1–41, 2004.

[37] Antoni Ivorra. *Bioimpedance monitoring for physicians : an overview*. PhD thesis, 2002.

[38] Carolina Hathenher Rodrigues and José de los Santos Guerra. *Implementação da técnica de espectroscopia de impedâncias para o estudo de propriedades físicas em materiais ferroelétricos*. PhD thesis, Universidade Federal de Uberlândia, Uberlândia - Minas Gerais, 2015.

[39] Mário Ferreira Alves. ABC dos circuitos eletricos em corrente alternada, 1999.

[40] Dennis Feucht. Z Meter on a Chip? Impedance Meter Bridge Circuits. http://www.planetanalog.com/author.asp?section_id=3049&doc_id=560900. Accessed August 21, 2016.

[41] Sen-ben Liao, Peter Dourmashkin, and John Belcher. *Chapter 11 Inductance and Magnetic Energy*. 2004.

[42] Geek3. https://commons.wikimedia.org/wiki/File:VFPt_cylindrical_magnet.svg. Accessed August 20, 2016.

[43] Michael W. Vogel, Andrea Giorni, Viktor Vegh, Ruben Pellicer-Guridi, and David C. Reutens. Rotatable Small Permanent Magnet Array for Ultra-Low Field Nuclear Magnetic Resonance Instrumentation: A Concept Study. pages 1–24, 2016.

[44] Mehmet Handi Kural, Serdar Celik, and Sainath Nageshwaran. Optimization of Cylindrical Halbach Permanent Magnet Array Dimensions for Magnetic Refrigeration. *Int. Refrigeration and Air Conditioning Conference*, pages 2335(1–7), 2010.

[45] R. Bjork, C. R H Bahl, A. Smith, and N. Pryds. Optimization and improvement of Halbach cylinder design. *Journal of Applied Physics*, 104(1), 2008.

[46] Peter Blumler. *Permanent Magnet System for MRI with Constant Gradient mechanically adjustable in Direction and Strength*. PhD thesis.

[47] Henley Court Pullman. Analog Discovery Technical Reference Manual Architectural Overview and Block Diagram. pages 1–39, 2015.

[48] Ltd Astrosyn International Technology. Stepping Motor type Y129 Technical Data.

[49] Innovative Sensor Technology. Application note RDT Platinum sensor, 2010.

[50] Analog Discovery. Digilent. www.reference.digilentinc.com. Accessed August 26, 2016.

[51] Sigma-Aldrich. PBS Sigma-Aldrich Product Specification.

[52] Hiroshi Abe, Masami Aono, and Yukihiro Yoshimura. Impedance Spectroscopic Study on Room Temperature Ionic Liquid-Water Mixtures. *J. Chem. Chem. Eng.*, 6:383–390, 2012.

[53] Song Hi Lee and Jayendran C. Rasaiah. Molecular dynamics simulation of ionic mobility. I. Alkali metal cations in water at 25 C. *The Journal of chemical physics*, 101(8):6964–6974, 1994.

[54] Peter Atkins and Julio de Paula. *Physical Chemistry, Eighth Edition*, volume 41. 2012.

[55] Ahmed Riaz and Reifsnider Ken. Study of influence of electrode geometry on impedance spectroscopy. *Int. J. Electrochem. Sci*, 2011.

[56] INC Plastic Products. PET(polyethylene terephalate) Typical Property Values. http://www.plastic-products.com/part12.htm. Accessed August 20, 2016.